Electronic Supplementary Information

Heterogeneous Photocatalytic Anaerobic Oxidation of Alcohols to Ketones by Pt-Mediated Hole Oxidation

Danhui Sun,[a,†] Peihe Li,[a†*] Xia Wang,[a] Yingying Wang,[a] Jinghui Wang,[a] Yin Wang,[a] Ye Lu,[a]

Limei Duan,[a*] Sarina Sarina,[b] Huaiyong Zhu[b] and Jinghai Liu[a*]

[a]*Inner Mongolia Key Laboratory of Carbon Nanomaterials, Nano Innovation Institute (NII), College of Chemistry and Materials Science, Inner Mongolia University for Nationalities, Tongliao, 028000, China.*
[b]*School of Chemistry, Physics and Mechanical Engineering, Queensland University of Technology, Brisbane, QLD 4001, Australia.*

E-mail: phli2018@foxmail.com, duanlmxie@126.com, jhliu2008@sinano.ac.cn.

1. Characterizations

All commercially available reagents were used without further purification. Unless stated otherwise, all reactions were carried out in Schlenk tube (25 mL) under nitrogen atmosphere. A 300 W Xe lamp (CEL-PE300-T8, Beijing Zhongjiao Jinyuan Technology Co., Ltd. Beijing, China. λ = 300-800 nm) was used as a light source. Column chromatography was performed on silica gel (200-400 mesh). GC analyses were performed on a Shimadzu GC-2014 equipped with a capillary column (HP-5 30 m × 0.25 μm × 0.32mm) using a flame ionization detector. Another gas chromatography (CEL-SPH2N-D9) was used for the detection of H_2. Melting points were determined using an SGWX-4 apparatus and are uncorrected. NMR spectra were taken with a Bruker 500 spectrometer at 500 MHz (^{1}H) and 125 MHz (^{13}C) using $CDCl_3$ as the solvent with TMS as internal standard.

The as-prepared samples were characterized by powder X-ray diffraction (XRD) on a SmartLab 9 kW (Rigaku, Cu Kα λ = 1.5406 Å). FT-IR spectra were performed on Nicolet 6700 IR spectrometer by using KBr plates. Ultraviolet–visible diffuse reflectance spectra (UV-Vis DRS) were recorded on Agilent Cary 300 with integrating sphere attachment ($BaSO_4$ as a reflectance standard). X-ray photoelectron spectra (XPS) were acquired on an ESCALAB Xi+ X-ray photoelectron spectrometer using Al Kα as the excitation source. The morphologies of the products were examined by scanning electron microscopy (SEM) using an S4800 scanning electron microscope (Hitachi). HRTEM, HAADF-scanning transmission electron microscopy (STEM) images and elemental mappings were obtained using a JEM2100F transmission electron microscope at an accelerating voltage of 200 kV (JEOL). The electrochemical analysis was carried out in a conventional three electrode cell using a Pt plate and an Ag/AgCl electrode as the counter electrode and reference electrode, respectively. The electrolyte was 0.2 M Na_2SO_4 aqueous solution without additives. The working electrode was prepared on glassy carbon electrode. 8 mg sample was dispersed in a mixture of ethanol and naphthol by sonication to get a slurry. N_2 adsorption-desorption isotherms were recorded on Quadrasorb SI Automated Surface area and Pore size analyzer (Quantachrome).

Computational Method. All the density functional theory (DFT) calculations were performed at the B3LYP level [1], with use of a standard 6-311++G(d, p) [2] basis set (Lanl2DZ basis set for Pt) [3] with Gaussian 09.[4] The geometry optimizations as well as HOMO and LUMO clouds of system were got by using the computer software Gauss View 05.

2. Materials and methods

2.1 Material Synthesis.

All chemicals are analytical grade and used as received without further purification.

2.2 Preparation of Pt/g-C_3N_4.

The graphitic carbon nitride (g-C_3N_4) was prepared using the same method that we had previously reported.[5] Briefly, urea (20 g, AR, Sinopharm Chemical Reagent Co., Ltd) was put in a crucible with a cover under ambient pressure in air. After thermal treatment at 550 ˚C for 3 hours, the mixture was washed with HNO_3 (0.1 M, 10 ml × 3), H_2O (10 ml × 3). The obtained compound g-C_3N_4 was dried under vacuum at 80 ˚C overnight (yellow solid, 800 mg).

Pt/g-C_3N_4 was prepared by a modified photo-deposition method. The certain amount of $H_2PtCl_6 \cdot 6H_2O$ (10 mg/mL, 0.3 mL) and acetic acid (1 mg/mL, 2 mL) were added into 100 mL g-C_3N_4 dispersion (deionized H_2O). After bubbling N_2 for half an hour, the sample was irradiated by a 300 W Xe lamp for an hour. The mixture was filtered and washed with H_2O (5 ml × 3). The obtained compound Pt/g-C_3N_4 was dried under vacuum at 80 ˚C overnight (yellow solid). (The preparation method of Pd/g-C_3N_4 and Ru/g-C_3N_4 are same as Pt/g-C_3N_4 with Na_2PdCl_4 and $RuCl_3$, respectively.)

2.3 Preparation of Fe/g-C_3N_4.

For preparation of the Fe/g-C_3N_4 photocatalysts, a certain amount of $Fe(NO_3)_3$ (0.5 mmol, 90 mg) was dissolved in 100 ml deionized water, 100 mg g-C_3N_4 was added. After stirring for half an hour, the solution was ultrasonically dispersed for 2 hours. The mixture was filtered and washed with H_2O (5 ml × 3). The obtained compound Fe/g-C_3N_4 was dried under vacuum at 80 ˚C overnight (yellow solid). (The preparation method of Cu/g-C_3N_4 is same as Fe/g-C_3N_4 with $Cu(NO_3)_3$.)

3. Evaluation of photocatalytic activity.

The reaction was performed in a 25 mL Schlenk bottle with 3 mL CH_3CN containing 5 mg Pt/g-C_3N_4 photocatalyst and 0.2 mmol benzhydrol. The reactor was sealed, degassed with N_2 for several times and then irradiated under simulated sunlight (300W Xe lamp). The temperature of the reaction system was kept at 25-35 ºC by a fan. After completion of the reaction, the generated gas was analyzed by gas chromatography immediately. The reaction mixture was centrifuged to remove the photocatalyst and the filtrate was concentrated in vacuo. The resulting residue was purified by silica gel flash chromatography (eluent: petroleum ether/ethyl acetate = 20:1) to give the product **2a** as a white solid (35 mg, 97% yield). In the recycle experiments, the catalyst was filtered after the reaction and washed with CH_3CN and dried under vacuum at 50 °C and used for the next cycle.

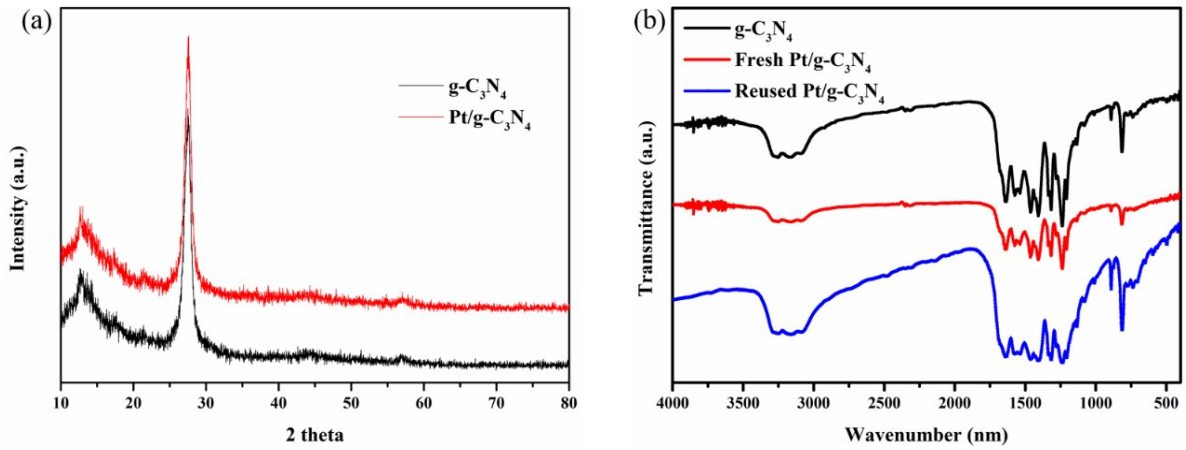

Fig. S1 (a) XRD patterns of prepared g-C_3N_4 and Pt/g-C_3N_4 samples. (b) FT-IR patterns of prepared g-C_3N_4, Fresh and Reused Pt/g-C_3N_4 samples.

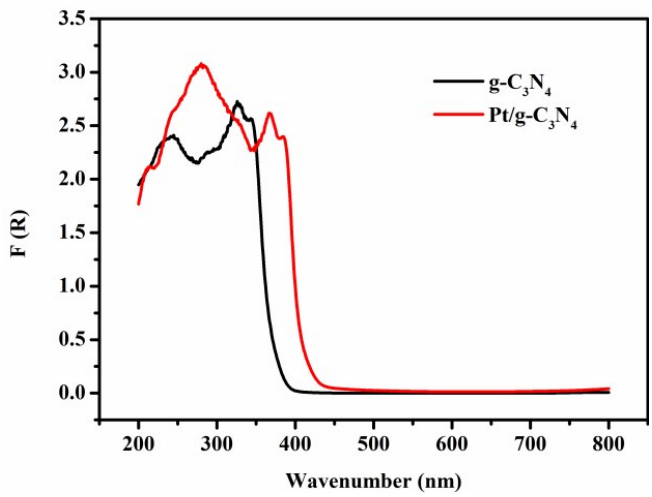

Fig. S2 UV-Vis DRS spectrum of g-C_3N_4 and Pt/g-C_3N_4 samples.

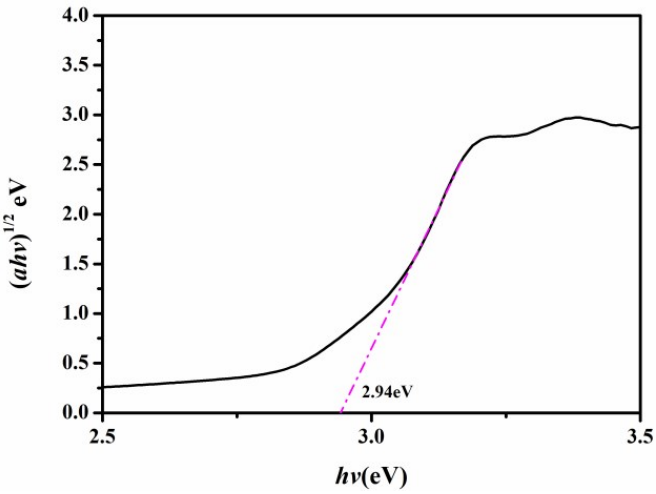

Fig. S3 Band gap of Pt/g-C_3N_4 obtained from the UV/Vis DRS spectrum according to the Kubelka–Munk theory.

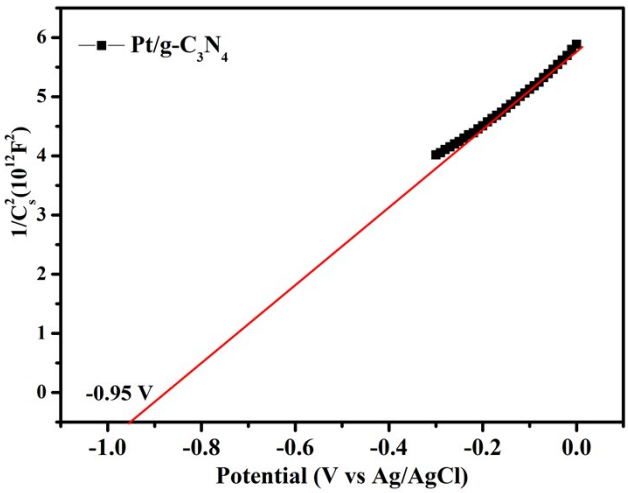

Fig. S4 Mott–Schottky plots.

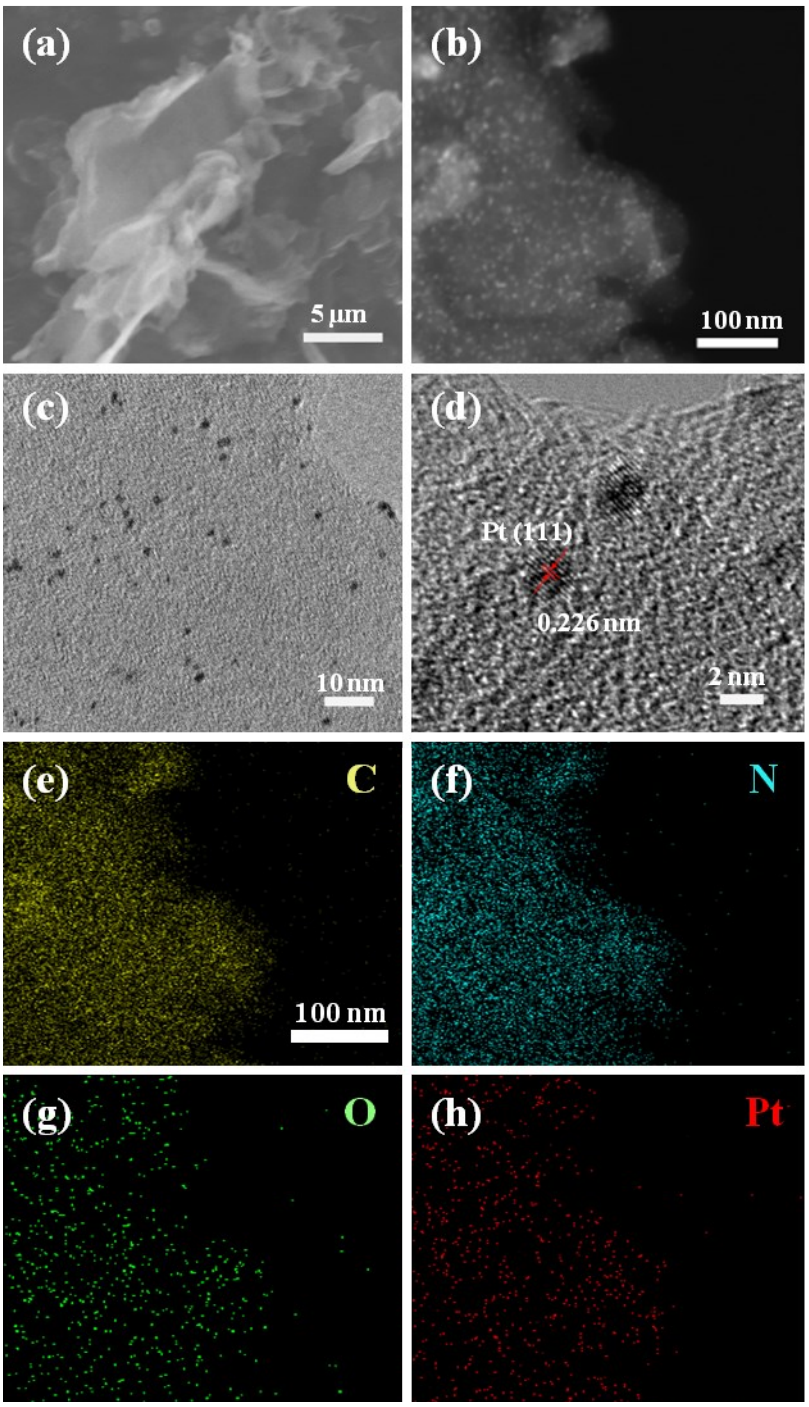

Fig. S5 (a) SEM image of Pt/g-C_3N_4, (b) STEM image of Pt/g-C_3N_4, (c) and (d) HRTEM images of Pt/g-C_3N_4, (e-h) the element mapping images of Pt/g-C_3N_4.

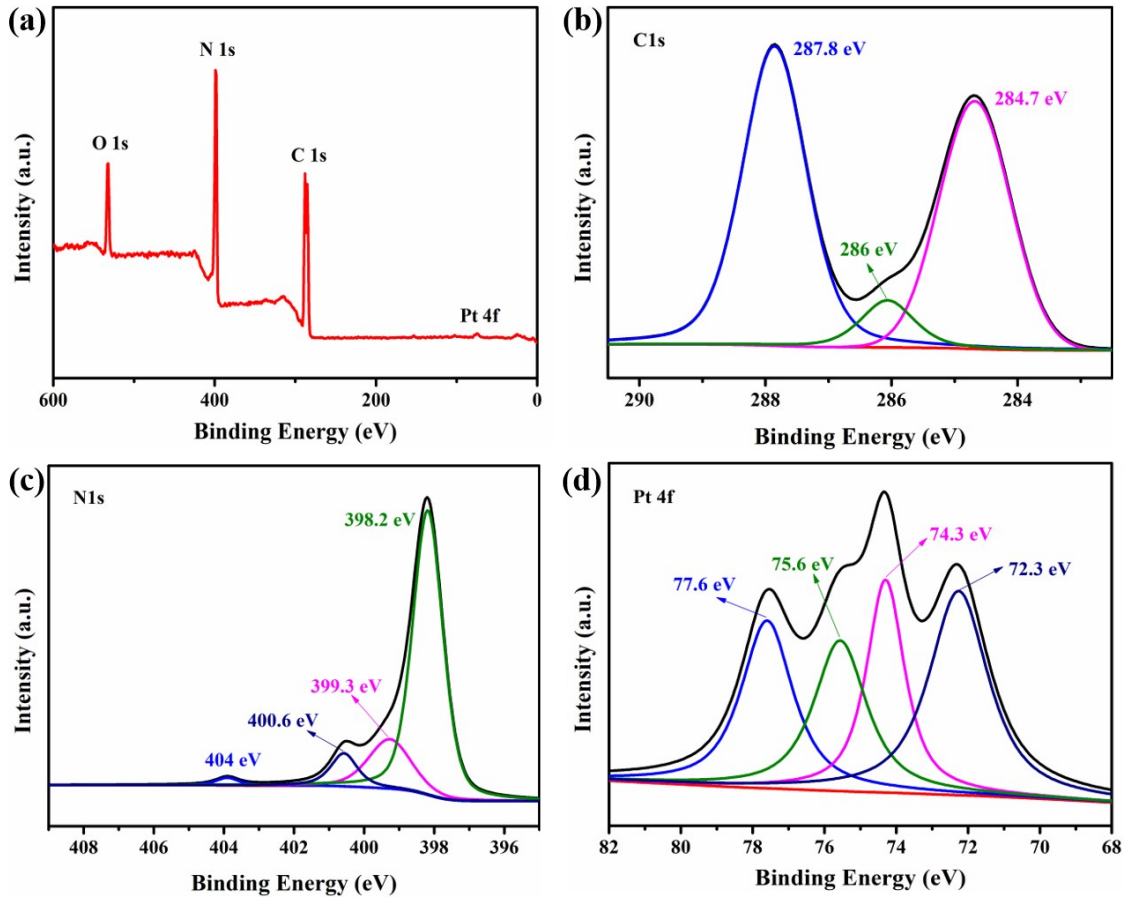

Fig. S6 XPS spectra of Pt/g-C_3N_4. (a) survey spectrum. High-resolution XPS spectra of (b) C 1s, (c) N 1s, (d) Pt $4f_{5/2}$ (77.6 eV, 75.6 eV), Pt $4f_{7/2}$ (74.3 eV, 72.3 eV).

The microstructure of the platinum nanocluster in Pt/g-C_3N_4 was examined by high-resolution transmission electron microscopy (HRTEM) and scanning transmission electron microscopy (STEM), where Pt nanoclusters with a size of about 2–3 nm were highly dispersed on the surface of g-C_3N_4 (Fig. S5, ESI†). The high-resolution Pt 4f XPS spectra reveal two valence states in the Pt nanocluster for the fresh Pt/g-C_3N_4 composite solid with Pt $4f_{5/2}$ at 77.6 eV (Pt^{4+}) and 75.6 eV (Pt^{2+}) and Pt $4f_{7/2}$ at 74.3 eV (Pt^{4+}) and 72.3 eV (Pt^{2+}) (Fig. S6, ESI†). The photophysical properties and the bandgap structure of Pt/g-C_3N_4 were further characterized to show its thermodynamic potential for solar-driven photocatalysis (Fig. S2–S4, ESI†).

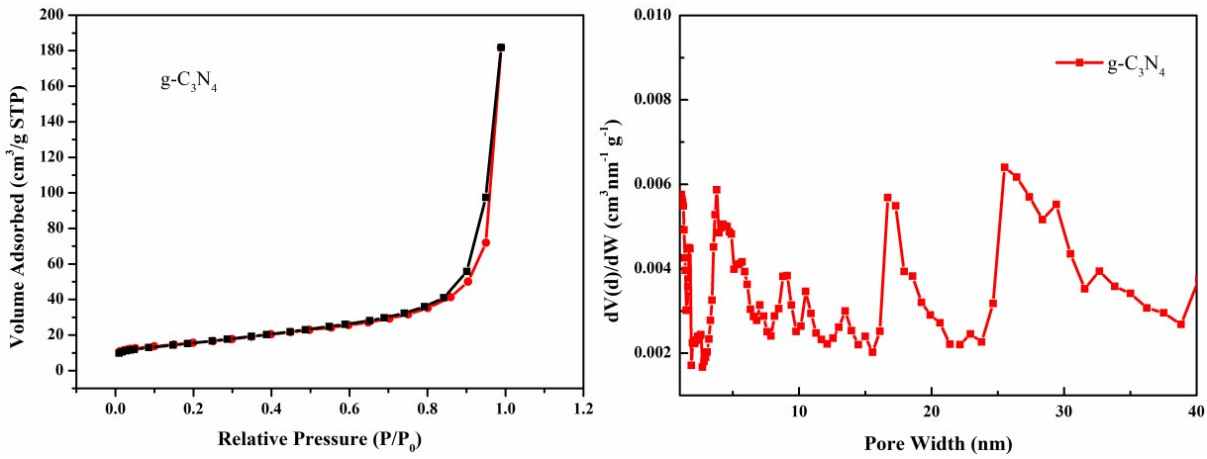

Fig. S7 (a) N_2 adsorption-desorption isotherms for g-C_3N_4, where BET surface area: 52.535 m^2/g. (b) Pore size distribution.

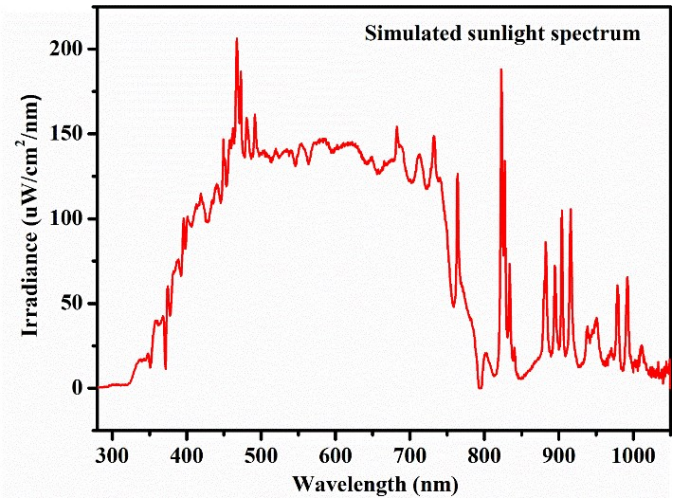

Fig. S8 The spectrum of simulated solar spectrum

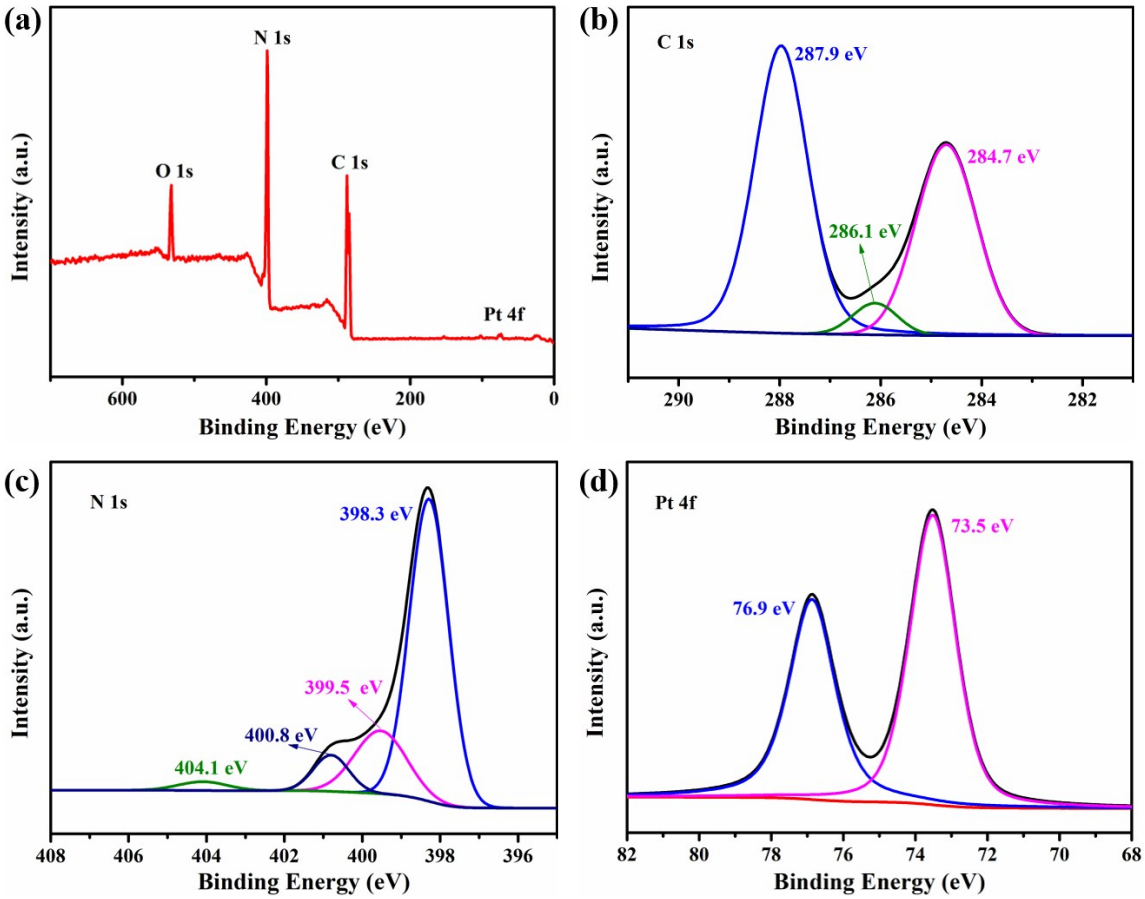

Fig. S9 XPS spectra of recovered Pt/g-C_3N_4. (a) survey spectrum. High-resolution XPS spectra of (b) C 1s, (c) N 1s, (d) Pt 4f, Pt $4f_{5/2}$ (76.9 eV), Pt $4f_{7/2}$ (73.5 eV).

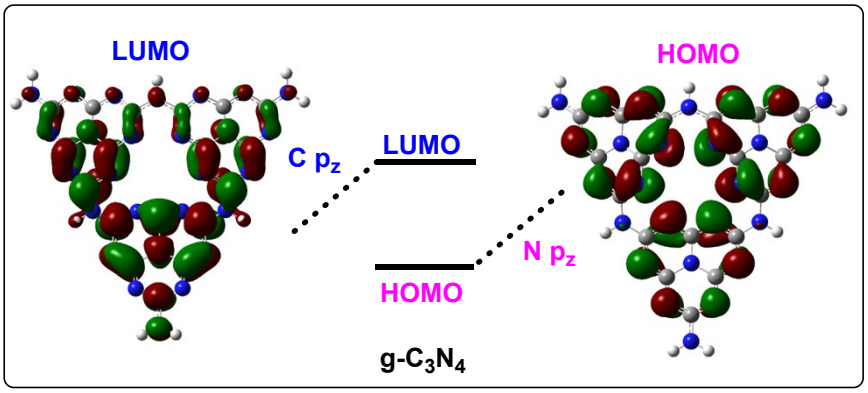

Fig. S10 DFT calculation for electronic structure of g-C_3N_4.

4. Kinetic isotope effect (KIE) experiment.

The reaction was performed in a 25 mL Schlenk bottle with 3 mL CH_3CN containing 5 mg Pt/g-C_3N_4 photocatalyst and 0.2 mmol cyclohexanol or cyclohexanol-D12 (CAS: 66522-78-9). The reactor was sealed, degassed with N_2 for several times and then irradiated under simulated sunlight (300W Xe lamp). The temperature of the reaction system was kept at 25-35 ºC by a fan. After completion of the reaction, the mixture was analyzed by gas chromatography (X: the peak area ratio of the product to the internal standard).

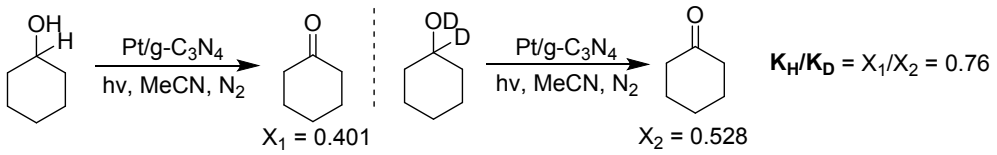

5. Quantum efficiency calculations.

The QE determination at λ_0 = 420 nm. The catalyst solution was irradiated by a 300W Xe lamp with a λ_0±20 nm band-pass filter for 15 hours. The average intensity of irradiation was determined to be 1.915 mW/cm^2 by an ILT 950 spectroradiometer (International Light Technologies) and the irradiation area was 6.12 cm^2. The number of incident photons (N) is 1.337×10^{21} as calculated by equation (1). The amount of H_2 molecules generated in 15 hours was 122.5 μmol (by GC). The quantum efficiency is calculated from equation (2).

$$N = \frac{E\lambda}{hc} = \frac{1.915 \times 10^{-3} \times 6.12 \times 15 \times 3600 \times 420 \times 10^{-9}}{6.626 \times 10^{-34} \times 3 \times 10^{8}} \left(\frac{W/cm^2 \times cm^2 \times s \times m}{J \cdot s \times m/s} \right) = 1.337 \times 10^{21} \quad \textbf{(1)}$$

$$QE = \frac{2 \times \text{the number of evolved } H_2 \text{ molecules}}{\text{the number of incident photons}} \times 100\%$$

$$= \frac{2 \times 6.02 \times 10^{23} \times 122.5 \times 10^{-6}}{1.337 \times 10^{21}} \times 100\% = 11.03\% \quad \textbf{(2)}$$

Spectroscopic data of products

Table 2, entry 1

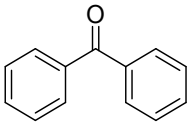

2a

Benzophenone (2a). Oil (35 mg, 97% yield); R_f = 0.35 (hexane: EtOAc = 20:1); ^{1}H NMR (500 MHz, $CDCl_3$) δ 7.81 (d, J = 5.2 Hz, 4H), 7.59 (t, J = 7.4 Hz, 2H), 7.49 (t, J = 7.7 Hz, 4H); ^{13}C NMR (125 MHz, $CDCl_3$) δ 197.2, 138.0, 132.8, 130.5, 128.7.

(1) S. Li, B. Zhu, R. Lee, B. Qiao, Z. Jiang, *Org. Chem. Front.,* 2018, **5**, 380–385.

Table 2, entry 2

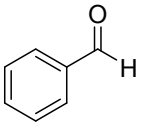

2b

Benzaldehyde (2b). Oil (19 mg, 89% yield); R_f = 0.35 (hexane: EtOAc = 20:1); ^{1}H NMR (500 MHz, $CDCl_3$) δ 10.05 (s, 1H), 7.91 (d, J = 7.0 Hz, 2H), 7.66 (t, J = 7.4 Hz, 1H), 7.56 (t, J = 7.6 Hz, 2H); ^{13}C NMR (125 MHz, $CDCl_3$) δ 192.5, 136.4, 134.5, 130.2, 129.8, 129.0, 128.5.

(1) S. Verma, R. B. N. Baig, M. N. Nadagouda, R. S. Varma, *ACS Sustainable Chem. Eng.,* 2016, **4**, 2333−2336.

Table 2, entry 3

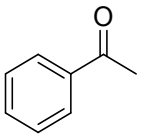

2c

Acetophenone (2c). Oil (18 mg, 75% yield); R_f = 0.4 (hexane: EtOAc = 20:1); ^{1}H NMR (500 MHz, $CDCl_3$) δ 7.97 (d, J = 7.2 Hz, 2H), 7.57 (t, J = 7.4 Hz, 1H), 7.47 (t, J = 7.7 Hz, 2H), 2.61 (s, 3H); ^{13}C NMR (125 MHz, $CDCl_3$) δ 197.9, 136.9, 132.9, 128.4, 128.1, 26.4.

(1) S. Li, B. Zhu, R. Lee, B. Qiao, Z. Jiang, *Org. Chem. Front.,* 2018, **5**, 380–385.

Table 2, entry 4

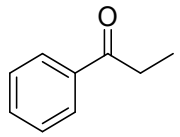

2d

Propiophenone (2d). Oil (18 mg, 67% yield); R_f = 0.35 (hexane: EtOAc = 20:1); ^{1}H NMR (500 MHz, $CDCl_3$) δ 7.99 (d, J = 8.0 Hz, 2H), 7.57 (t, J = 7.9 Hz, 1H), 7.47 (t, J = 7.6 Hz, 2H), 3.02 (q, J = 7.2 Hz, 2H), 1.25 (s, 3H); ^{13}C NMR (125 MHz, $CDCl_3$) δ 136.9, 132.9, 128.6, 127.9, 31.8, 26.5, 8.2.

(1) H. Peng, A. Lin, Y. Zhang, H. Jiang, J. Zhou, Y. Cheng, C. Zhu, H. Hu, *ACS Catal.,* 2012, **2**, 163−167.

Table 2, entry 5

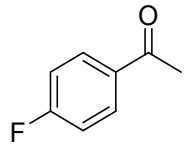

2e

1-(4-Fluoropheny)ethanone (2e). Oil (18 mg, 65% yield); R_f = 0.4 (hexane: EtOAc = 20:1); ^{1}H NMR (500 MHz, $CDCl_3$) δ 8.01 (dd, J = 7.4, 5.4 Hz, 2H), 7.16 (t, J = 8.0 Hz, 2H), 2.61 (s, 3H); ^{13}C NMR (126 MHz, $CDCl_3$) δ 196.5, 165.8 (d, $^1J_{C\text{-}F}$ = 254.6 Hz), 133.6 (d, $^4J_{C\text{-}F}$ = 2.9 Hz), 130.9 (d, $^3J_{C\text{-}F}$ = 9.3 Hz), 115.66 (d, $^2J_{C\text{-}F}$ = 21.9 Hz), 26.5.

(1) F. Li, N. Wang, L. Lu, G. Zhu, *J. Org. Chem.,* 2015, **80**, 3538−3546.

Table 2, entry 6

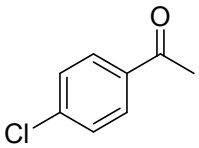

2f

1-(4-Chloropheny)ethanone (2f). Oil (24 mg, 76% yield); R_f = 0.4 (hexane: EtOAc = 20:1); ^{1}H NMR (500 MHz, $CDCl_3$) δ 7.89 (d, J = 8.6 Hz, 2H), 7.43 (d, J = 8.6 Hz, 2H), 2.59 (s, 3H); ^{13}C NMR (125 MHz, $CDCl_3$) δ 196.9, 139.7, 135.6, 129.9, 129.0, 26.7.

(1) S. Li, B. Zhu, R. Lee, B. Qiao, Z. Jiang, *Org. Chem. Front.,* 2018, **5**, 380–385.

Table 2, entry 7

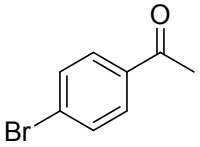

2g

1-(4-Bromopheny)ethanone (2g). Oil (32 mg, 80% yield); R_f = 0.33 (hexane: EtOAc = 20:1); ^{1}H NMR (500 MHz, $CDCl_3$) δ 7.80 (d, J = 8.5 Hz, 2H), 7.59 (d, J = 8.5 Hz, 2H), 2.57 (s, 3H); ^{13}C NMR (125 MHz, $CDCl_3$) δ 197.0, 135.8, 131.9, 129.9, 128.3, 26.6.

(1) S. Li, B. Zhu, R. Lee, B. Qiao, Z. Jiang, *Org. Chem. Front.,* 2018, **5**, 380–385.

Table 2, entry 8

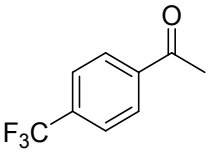

2h

4-(Trifluoromethyl) acetophenone (2h). Oil (31 mg, 82% yield); Rf = 0.4 (hexane: EtOAc = 20:1); ^{1}H NMR (500 MHz, $CDCl_3$) δ 8.08 (d, J = 8.1 Hz, 2H), 7.75 (d, J = 8.2 Hz, 2H), 2.67 (s, 3H); ^{13}C NMR (125 MHz, $CDCl_3$) δ 197.0, 139.7, 134.5 (q, $^2J_{C\text{-}F}$ = 32.5 Hz), 128.6, 125.7 (q, $^3J_{C\text{-}F}$ = 3.75 Hz), 124.0 (q, $^1J_{C\text{-}F}$ = 235 Hz), 26.8.

(1) F. Li, N. Wang, L. Lu, G. Zhu, *J. Org. Chem.,* 2015, **80**, 3538−3546.

Table 2, entry 9

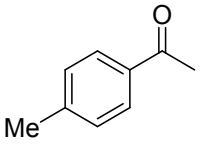

2i

1-(*p*-tolyl)ethanone (2i). Oil (18 mg, 68% yield); R_f = 0.33 (hexane: EtOAc = 20:1); ^{1}H NMR (500 MHz, $CDCl_3$) δ 7.87 (d, J = 8.1 Hz, 2H), 7.27 (d, J = 8.0 Hz, 2H), 2.59 (s, 3H), 2.42 (s, 3H); ^{13}C NMR (125 MHz, $CDCl_3$) δ 197.9, 143.9, 134.8, 129.3, 128.5, 26.6, 21.7.

(1) H. Peng, A. Lin, Y. Zhang, H. Jiang, J. Zhou, Y. Cheng, C. Zhu, H. Hu, *ACS Catal.,* 2012, **2**, 163−167.

Table 2, entry 10

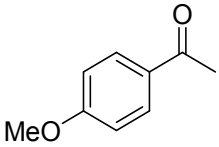

2j

1,1'-(1,4-phenylene)diethanone (2j). White solid (25 mg, 82% yield); mp:114-115 ℃; R_f = 0.33 (hexane: EtOAc = 20:1); ^{1}H NMR (500 MHz, $CDCl_3$) δ 7.94 (d, J = 8.7 Hz, 2H), 6.93 (d, J = 8.7 Hz, 2H), 3.87 (s, 3H), 2.55 (s, 3H); ^{13}C NMR (125 MHz, $CDCl_3$) δ 196.8, 163.4, 130.5, 130.3, 113.6, 55.4, 26.3.

(1) H. Peng, A. Lin, Y. Zhang, H. Jiang, J. Zhou, Y. Cheng, C. Zhu, H. Hu, *ACS Catal.,* 2012, **2**, 163−167.

Table 2, entry 11

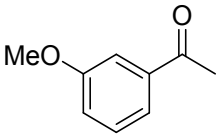

2k

1,1'-(1,3-phenylene)diethanone (2k). Oil (21 mg, 69% yield); R_f = 0.33 (hexane: EtOAc = 20:1); ^{1}H NMR (500 MHz, $CDCl_3$) δ 7.57–7.55 (m, 1H), 7.51 (dd, J = 2.5, 1.6 Hz, 1H), 7.39 (t, J = 7.9 Hz, 1H), 7.14 (ddd, J = 8.2, 2.7, 0.8 Hz, 1H), 3.88 (s, 3H), 2.62 (s, 3H); ^{13}C NMR (125 MHz, $CDCl_3$) δ 197.7, 159.5, 138.2, 129.3, 120.9, 119.4, 112.1, 55.2, 26.4.

(1) G. Zhang, S. K. Hanson, *Org. Lett.,* 2013, **15**, 650−653.

Table 2, entry 12

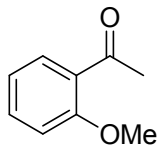

2l

1,1'-(1,2-phenylene)diethanone (2l). Oil (18 mg, 61% yield); R_f = 0.33 (hexane: EtOAc = 20:1); ^{1}H NMR (500 MHz, $CDCl_3$) δ 7.75 (dd, J = 7.7, 1.8 Hz, 1H), 7.49 (ddd, J = 8.5, 7.4, 1.8 Hz, 1H), 7.02 (t, J = 7.6 Hz, 1H), 6.99 (d, J = 8.4 Hz, 1H), 3.94 (s, 3H), 2.64 (s, 3H); ^{13}C NMR (125 MHz, $CDCl_3$) δ 199.9, 158.9, 133.7, 130.4, 128.3, 120.6, 111.6, 55.5, 31.8.

(1) G. Urgoitia, R. SanMartin, , M. T. Herrero E. Dominguez, *Green Chem.,* 2011, **13**, 2161−2166.

Table 2, entry 13

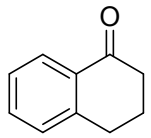

2m

3,4-dihydronaphthalen-1(2*H*)-one (2m). Oil (21 mg, 72% yield); R_f = 0.31 (hexane: EtOAc = 20:1); ^{1}H NMR (500 MHz, $CDCl_3$) δ 8.05 (d, J = 7.8 Hz, 1H), 7.48 (t, J = 8.1 Hz, 1H), 7.32 (t, J = 7.6 Hz, 1H), 7.27 (d, J = 7.7 Hz, 1H), 2.99 (t, J = 6.1 Hz, 2H), 2.78–2.60 (m, 2H), 2.23–2.06 (m, 2H); ^{13}C NMR (125 MHz, $CDCl_3$) δ 198.8, 144.8, 133.7, 133.0, 129.1, 127.5, 127.0, 39.5, 30.1, 23.6.

(1) G. Urgoitia, R. SanMartin, , M. T. Herrero E. Dominguez, *Green Chem.,* 2011, **13**, 2161−2166.

Table 2, entry 14

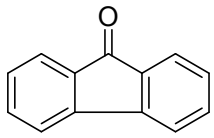

2n

9*H*-Fluoren-9-one (2n). Yellow solid (31 mg, 86% yield); mp: 81-82 ℃; R_f = 0.30 (hexane: EtOAc = 20:1); ^{1}H NMR (500 MHz, $CDCl_3$) δ 7.63 (d, J = 7.3 Hz, 2H), 7.46 (t, J = 7.0 Hz, 4H), 7.26 (dd, J = 9.6, 4.4 Hz, 2H); ^{13}C NMR (125 MHz, $CDCl_3$) δ 193.9, 144.4, 134.7, 134.1, 129.1, 124.3, 120.4.

(1) H. Peng, A. Lin, Y. Zhang, H. Jiang, J. Zhou, Y. Cheng, C. Zhu, H. Hu, *ACS Catal.,* 2012, **2**, 163−167.

Table 2, entry 15

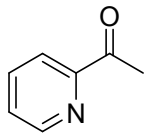

2o

1-(pyridin-2-yl)ethanone (2o). Oil (15 mg, 61%); R_f = 0.31 (hexane:EtOAc = 10:1); ^{1}H NMR (500 MHz, $CDCl_3$) δ 8.66 (d, J = 4.7 Hz, 1H), 8.01 (d, J = 7.9 Hz, 1H), 7.81 (t, J = 7.7 Hz, 1H), 7.45–7.43 (m, 1H), 2.70 (s, 3H); ^{13}C NMR (125 MHz, $CDCl_3$) δ 200.1, 153.5, 148.9, 136.8, 127.1, 121.6, 25.8.

(1) M. B. Lauber, S. S. Stahl, *ACS Catal.,* 2013, **3**, 2612−2616.

Table 2, entry 16

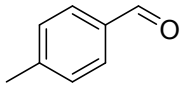

2p

4-methylbenzaldehyde (2p). Oil (22 mg, 93%); R_f = 0.61 (hexane:EtOAc = 10:1); ^{1}H NMR (500 MHz, $CDCl_3$) δ 9.94 (s, 1H), 7.75 (d, J = 8.1 Hz, 2H), 7.30 (d, J = 8.1 Hz, 2H), 2.41 (s, 3H); ^{13}C NMR (126 MHz, $CDCl_3$) δ 191.9, 145.5, 134.1, 129.8, 129.7, 21.8.

(1) X.-J. Yang, Y.-W. Zheng, L.-Q. Zheng, L.-Z. Wu, C.-H. Tung and B. Chen, *Green Chem*., 2019, **21**, 1401–1405.

Table 2, entry 17

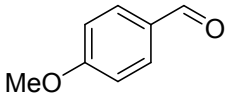

2q

4-methoxybenzaldehyde (2q). Oil (24 mg, 90%); R_f = 0.51 (hexane:EtOAc = 10:1); ^{1}H NMR (500 MHz, $CDCl_3$) δ 9.88 (s, 1H), 7.84 (d, J = 8.6 Hz, 2H), 7.00 (d, J = 8.7 Hz, 2H), 3.89 (s, 3H); ^{13}C NMR (126 MHz, $CDCl_3$) δ 190.8, 164.6, 131.9, 129.9, 114.3, 55.5.

(1) X.-J. Yang, Y.-W. Zheng, L.-Q. Zheng, L.-Z. Wu, C.-H. Tung and B. Chen, *Green Chem*., 2019, **21**, 1401–1405.

Table 2, entry 18

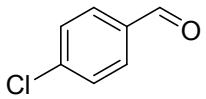

2r

4-chlorobenzaldehyde (2r). Oil (27 mg, 96%); R_f = 0.60 (hexane:EtOAc = 10:1); ^{1}H NMR (500 MHz, $CDCl_3$) δ 9.98 (s, 1H), 7.82 (d, J = 7.6 Hz, 2H), 7.51 (d, J = 7.9 Hz, 2H); ^{13}C NMR (126 MHz, $CDCl_3$) δ 190.8, 140.9, 134.7, 130.9, 129.4.

(1) X.-J. Yang, Y.-W. Zheng, L.-Q. Zheng, L.-Z. Wu, C.-H. Tung and B. Chen, *Green Chem*., 2019, **21**, 1401–1405.

Table 2, entry 19

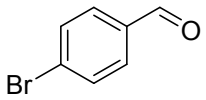

2s

4-bromobenzaldehyde (2s). White solid (35 mg, 95%); mp: 57-59 ℃; R_f = 0.55 (hexane:EtOAc = 10:1); ^{1}H NMR (500 MHz, $CDCl_3$) δ 9.99 (s, 1H), 7.76 (d, J = 8.3 Hz, 2H), 7.69 (d, J = 8.4 Hz, 2H); ^{13}C NMR (126 MHz, $CDCl_3$) δ 191.1, 135.0, 132.4, 130.9, 129.8.

(1) Z.Wei,S.Ru, Q. Zhao, H. Yu, G. Zhang, Y. Wei, *Green Chem*., 2019, **21**, 4069–4075.

Table 2, entry 20

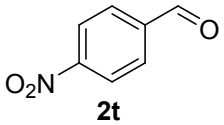

2t

4-nitrobenzaldehyde (2t). yellow solid (27 mg, 89%); mp: 105-106 ℃; R_f = 0.4 (hexane:EtOAc = 10:1); ^{1}H NMR (500 MHz, $CDCl_3$) δ 10.17 (s, 1H), 8.40 (dd, J = 8.5, 1.3 Hz, 2H), 8.09 (dd, J = 8.6, 1.5 Hz, 2H); ^{13}C NMR (126 MHz, $CDCl_3$) δ 190.3, 151.1, 140.0, 130.5, 124.3.

(1) Z.Wei,S.Ru, Q. Zhao, H. Yu, G. Zhang, Y. Wei, *Green Chem*., 2019, **21**, 4069–4075.

Table 2, entry 21

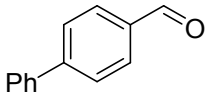

2u

[1,1'-biphenyl]-4-carbaldehyde (2u). White solid (29 mg, 80%); mp: 57-59 ℃; R_f = 0.55 (hexane:EtOAc = 10:1); ^{1}H NMR (500 MHz, $CDCl_3$) δ 10.08 (s, 1H), 7.97 (d, J = 8.3 Hz, 2H), 7.77 (d, J = 8.2 Hz, 2H), 7.70–7.64 (m, 2H), 7.51 (dd, J = 10.3, 4.7 Hz, 2H), 7.45 (dd, J = 8.4, 6.3 Hz, 1H). ^{13}C NMR (126 MHz, $CDCl_3$) δ 191.9, 147.2, 139.7, 135.2, 130.3, 129.0, 128.5, 127.7, 127.4.

Table 3, entry 6

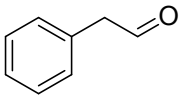

2aa

2-phenylacetaldehyde (2aa). Oil (21 mg, 89%); R_f = 0.65 (hexane:EtOAc = 10:1); ^{1}H NMR (500 MHz, $CDCl_3$) δ 9.77 (t, J = 2.4 Hz, 1H), 7.41 (t, J = 7.4 Hz, 2H), 7.35 (t, J = 7.4 Hz, 1H), 7.26 (d, J = 7.2 Hz, 2H), 3.72 (d, J = 2.3 Hz, 2H); ^{13}C NMR (126 MHz, $CDCl_3$) δ 199.5, 131.9, 129.6, 129.0, 127.4, 50.5.

Table 3, entry 7

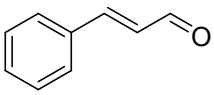

2ab

Cinnamaldehyde (2ab). Oil (14 mg, 52%); R_f = 0.60 (hexane:EtOAc = 10:1); ^{1}H NMR (500 MHz, $CDCl_3$) δ 9.71 (d, J = 7.7 Hz, 1H), 7.60–7.54 (m, 2H), 7.52–7.40 (m, 4H), 6.73 (dd, J = 16.0, 7.7 Hz, 1H); ^{13}C NMR (126 MHz, $CDCl_3$) δ 193.7, 152.8, 134.0, 131.3, 129.1, 128.5, 128.5.

(1) W. Huang, B. C. Ma, H. Lu, R. Li, L. Wang, K. Landfester and K. A. I. Zhang, *ACS Catal*., 2017, **7**, 5438–5442

^{1}H NMR and ^{13}C NMR Spectrum of **2a**

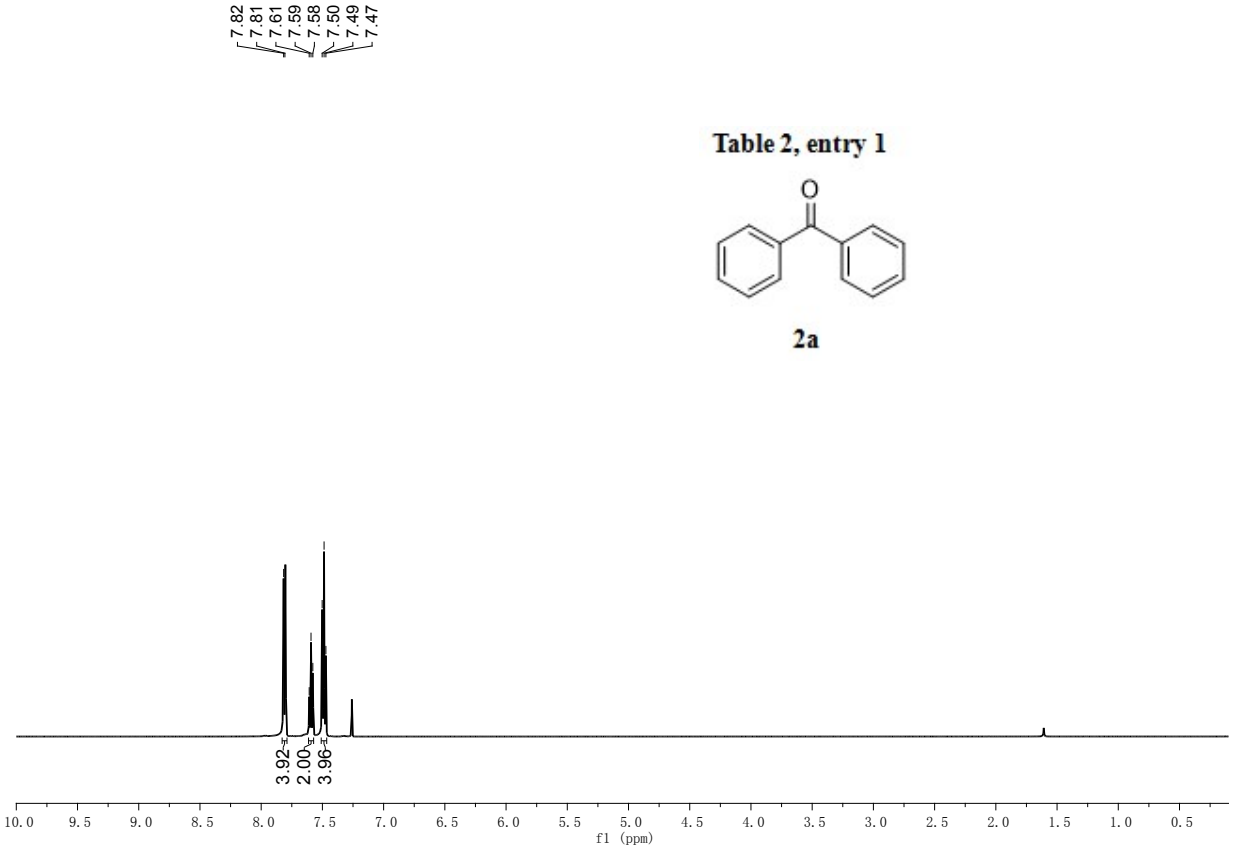

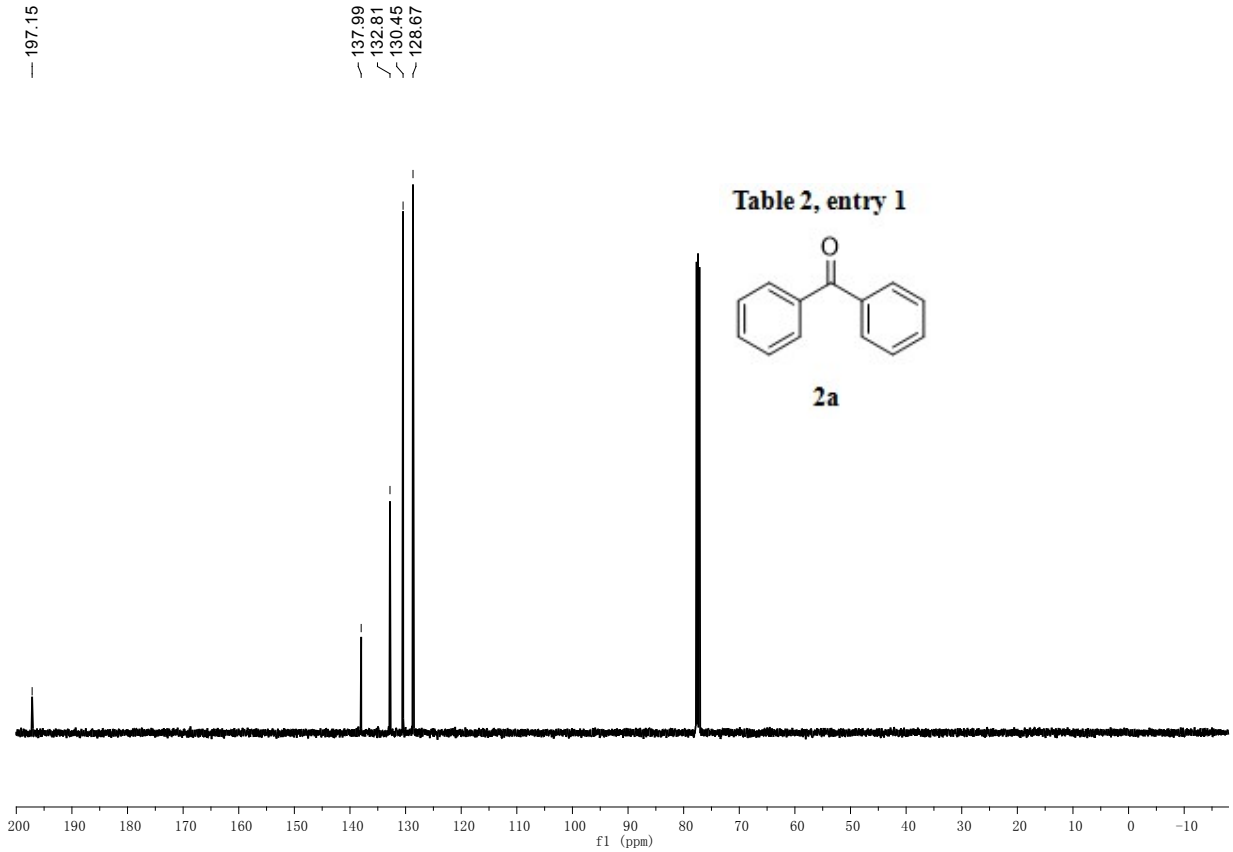

^{1}H NMR and ^{13}C NMR Spectrum of **2b**

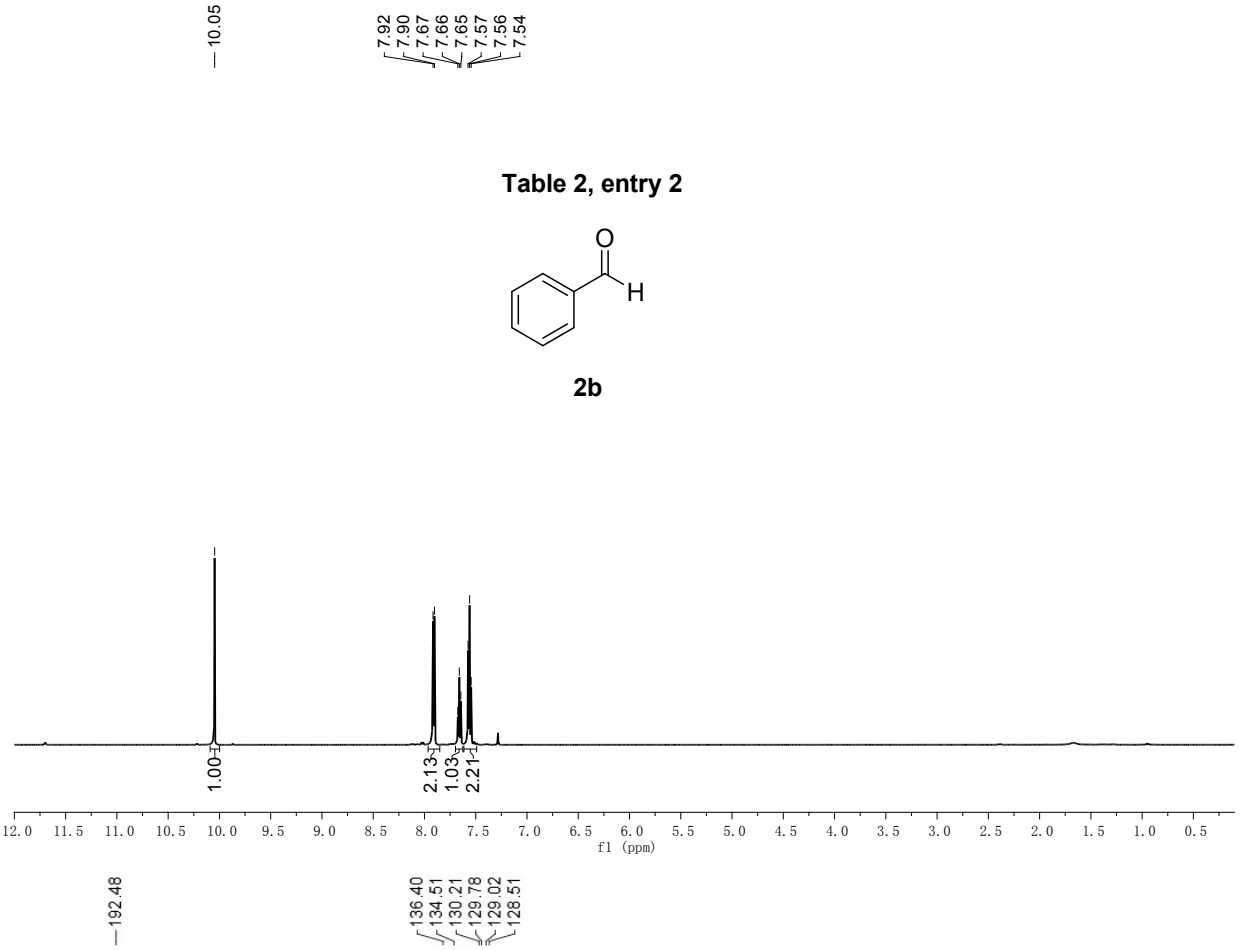

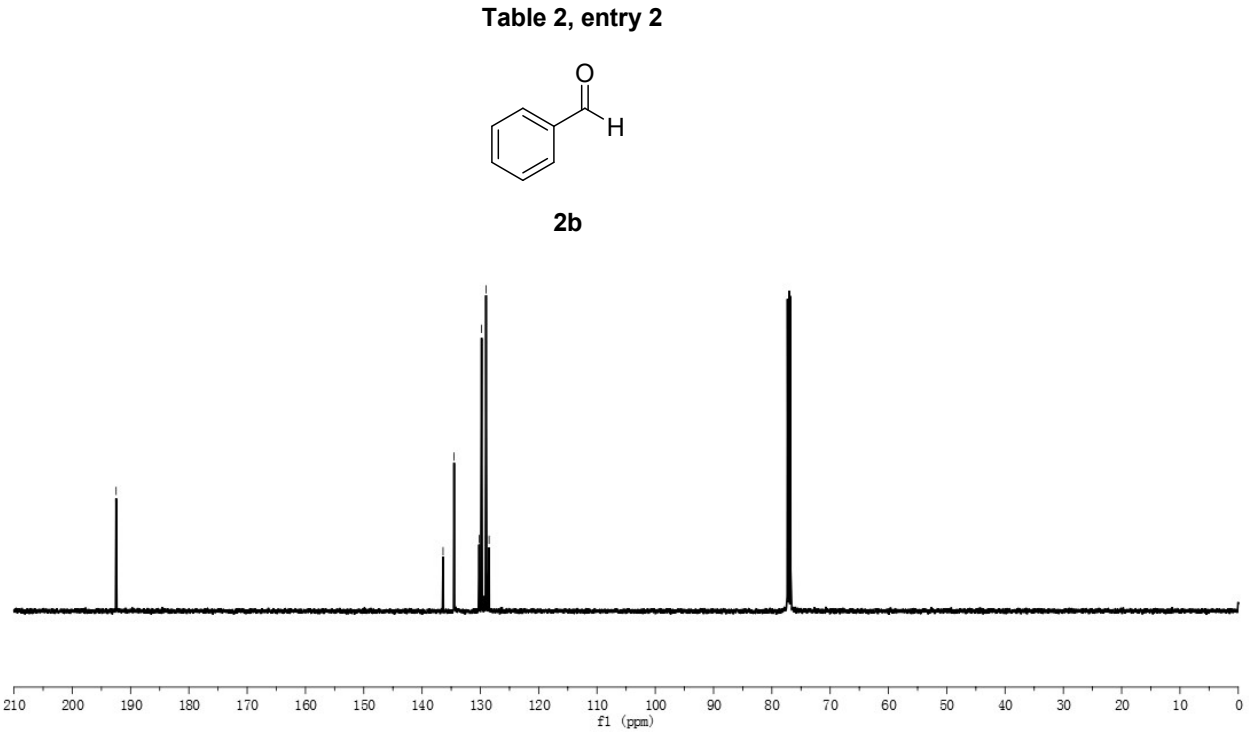

^{1}H NMR and ^{13}C NMR Spectrum of **2c**

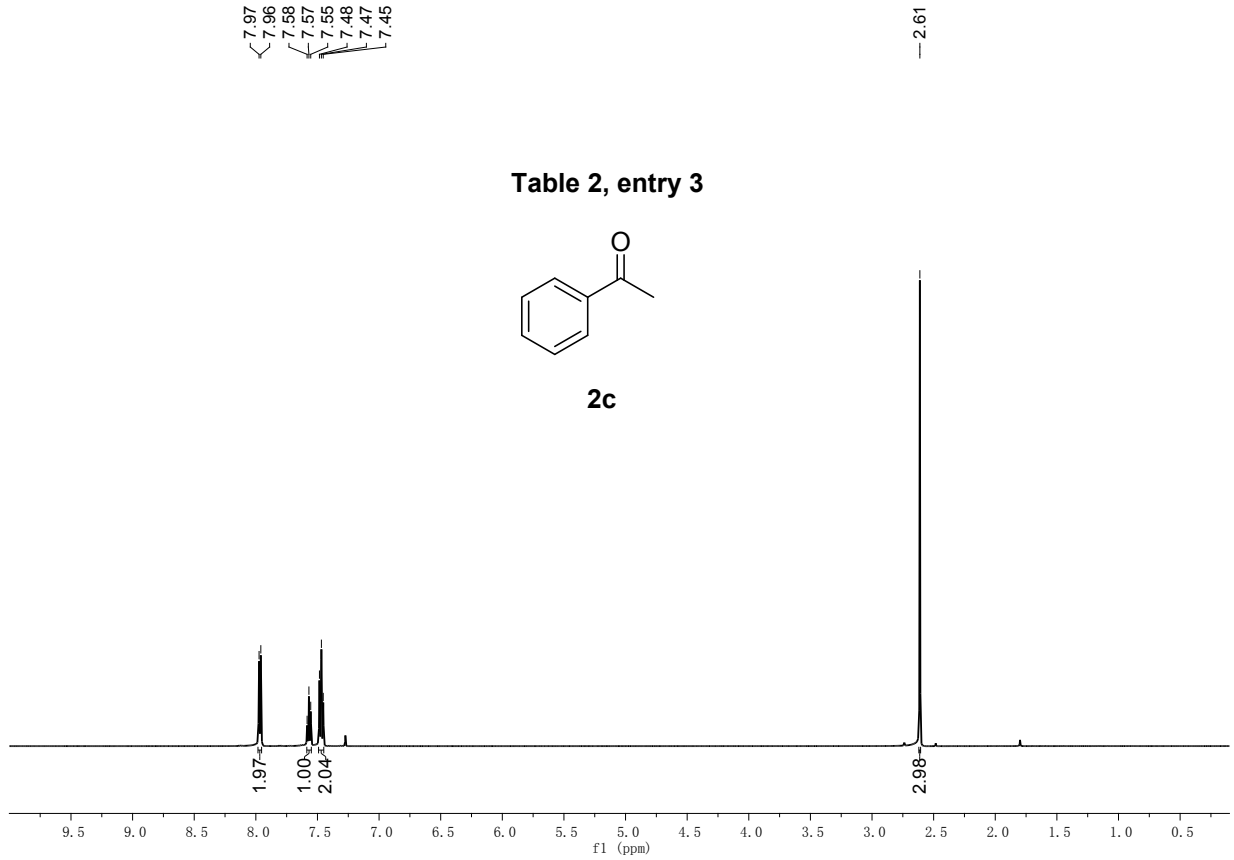

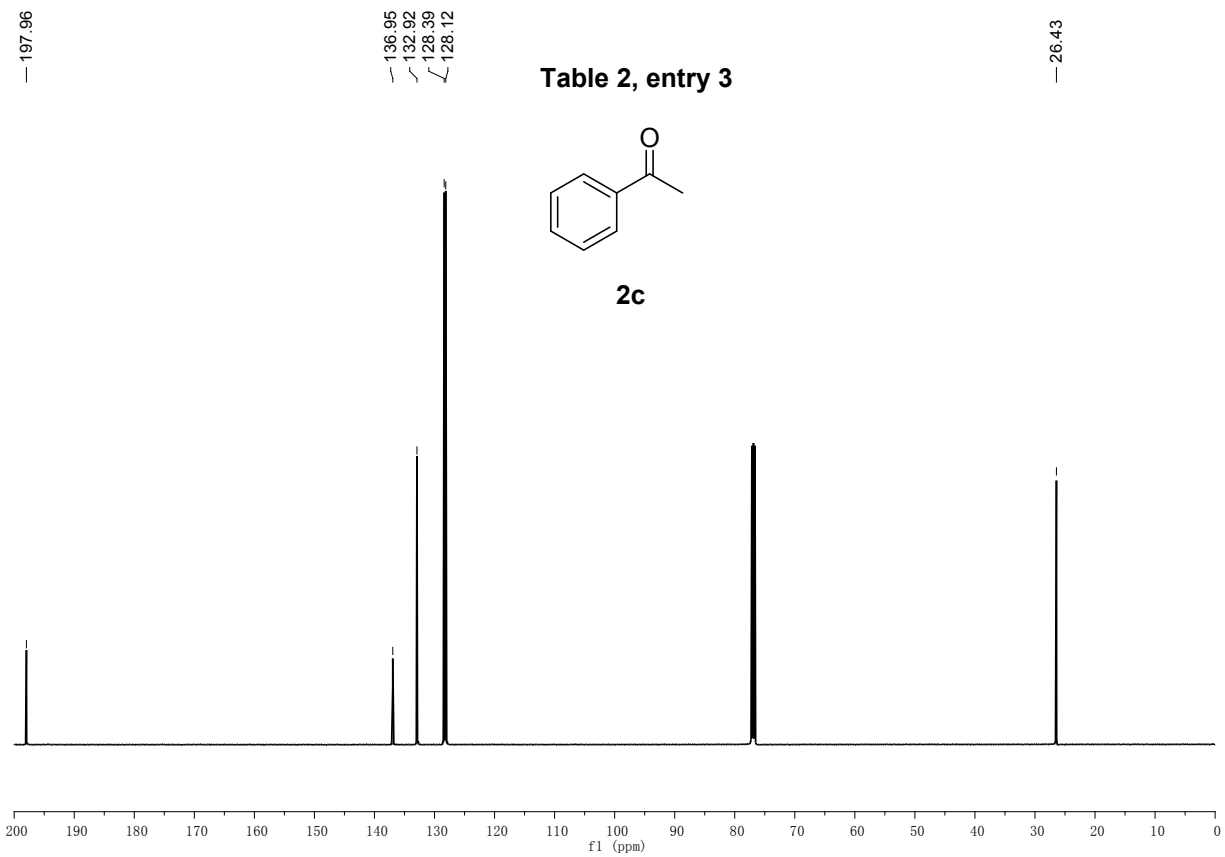

^{1}H NMR and ^{13}C NMR Spectrum of **2d**

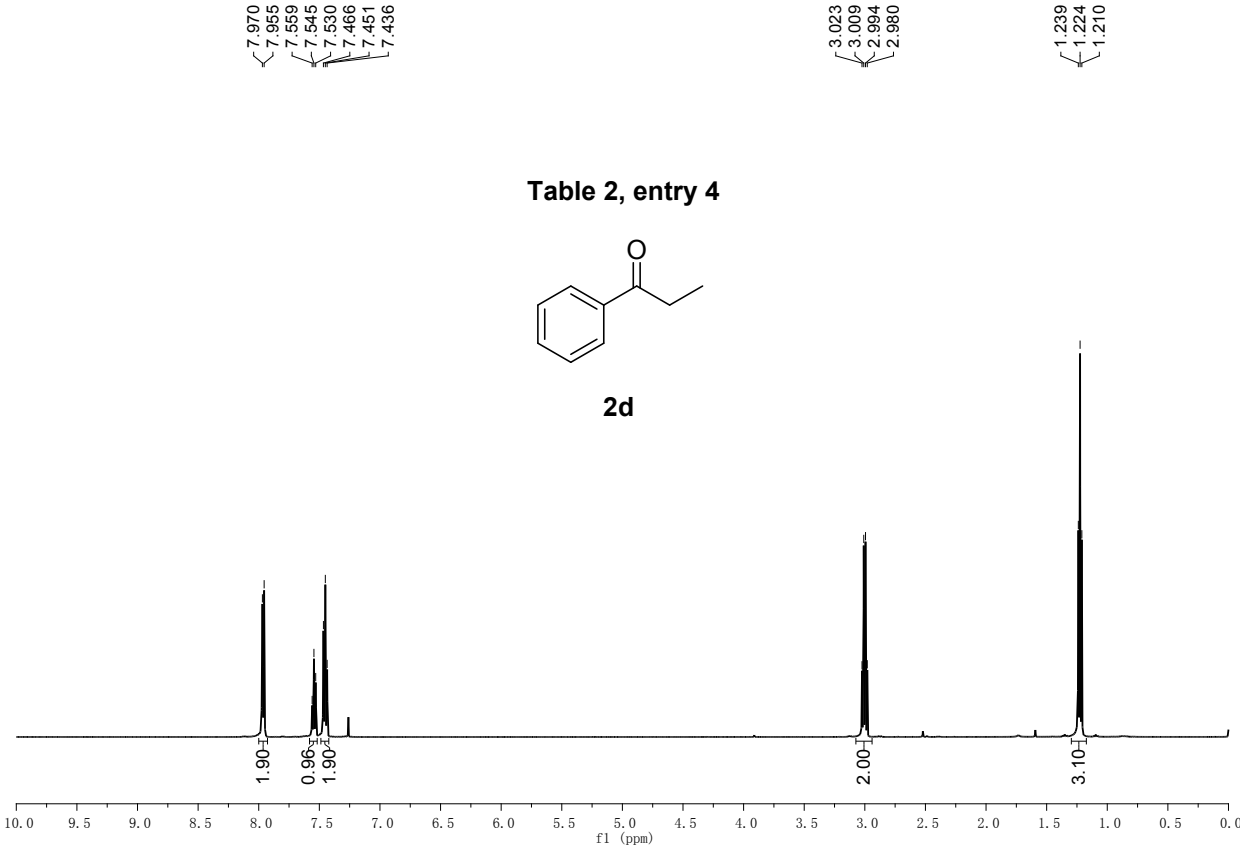

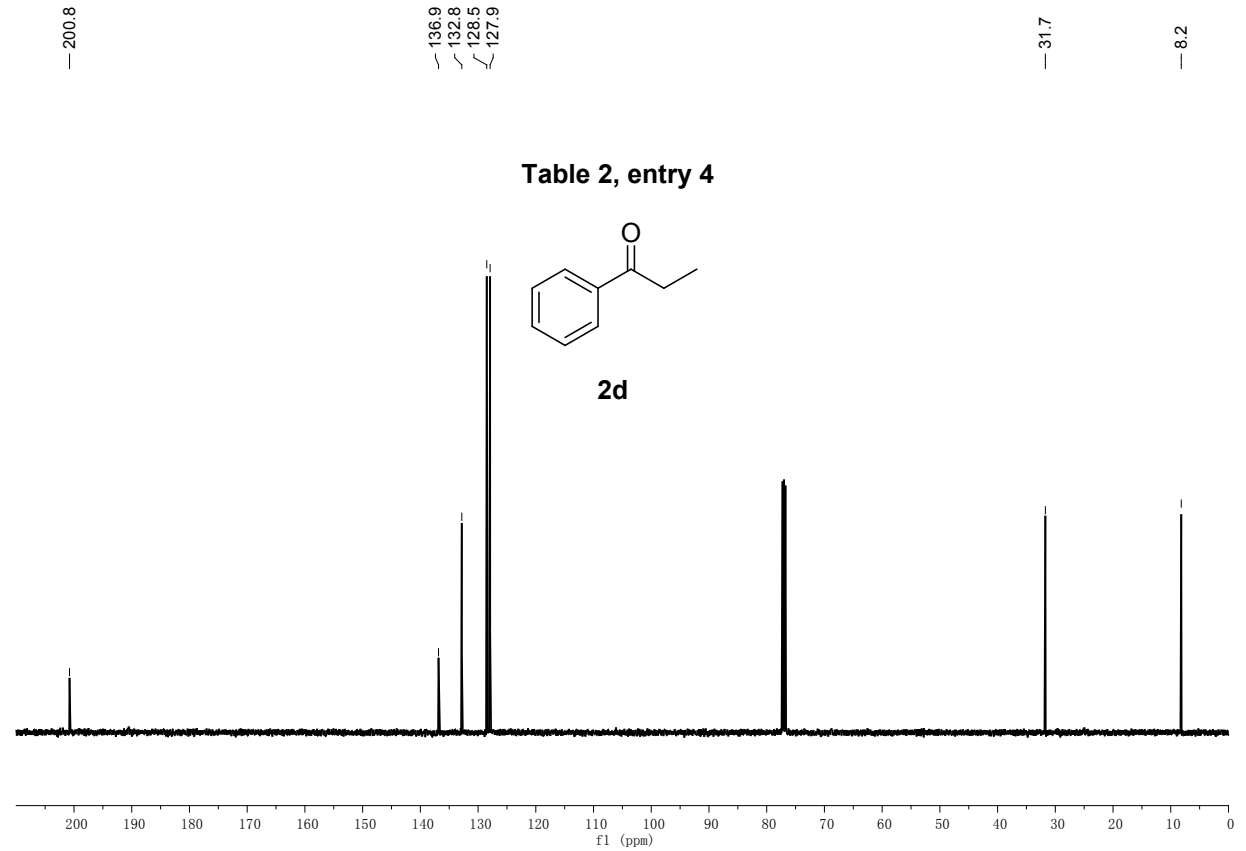

^{1}H NMR and ^{13}C NMR Spectrum of **2e**

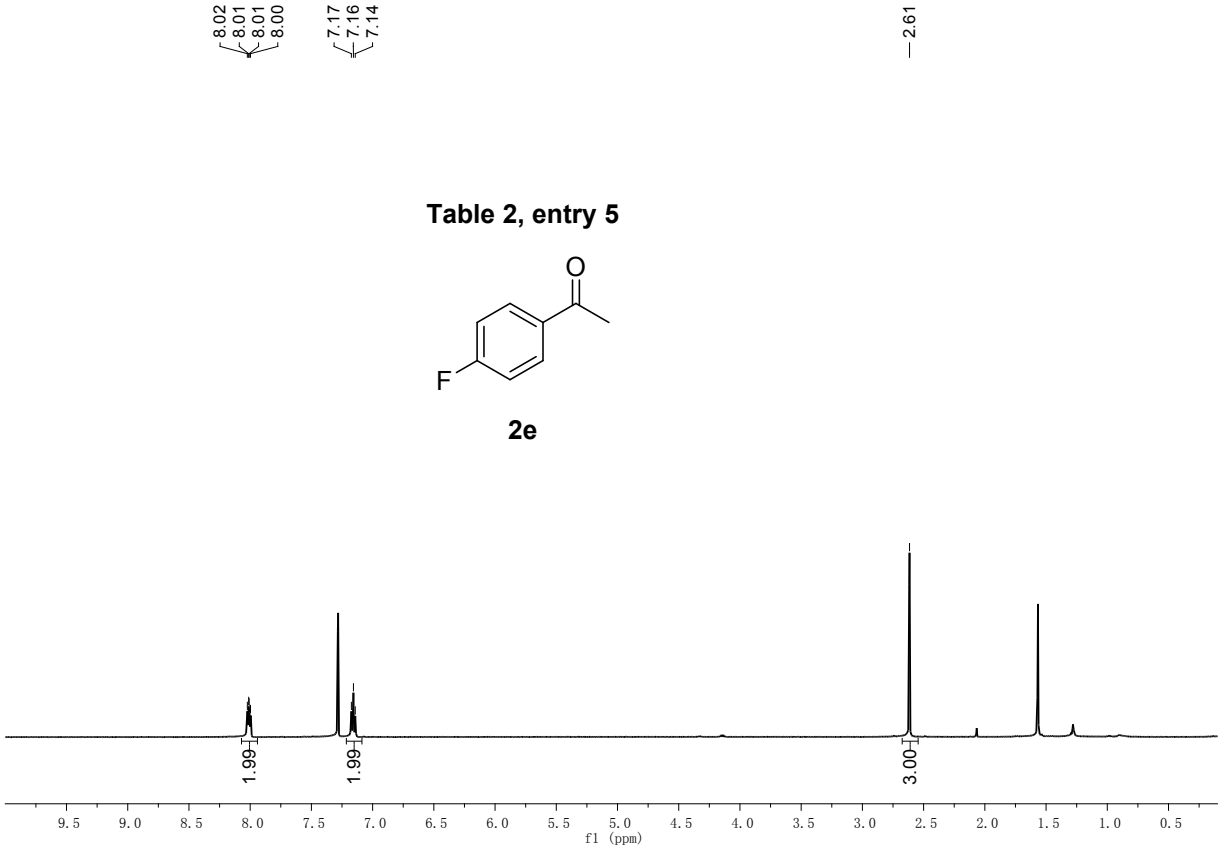

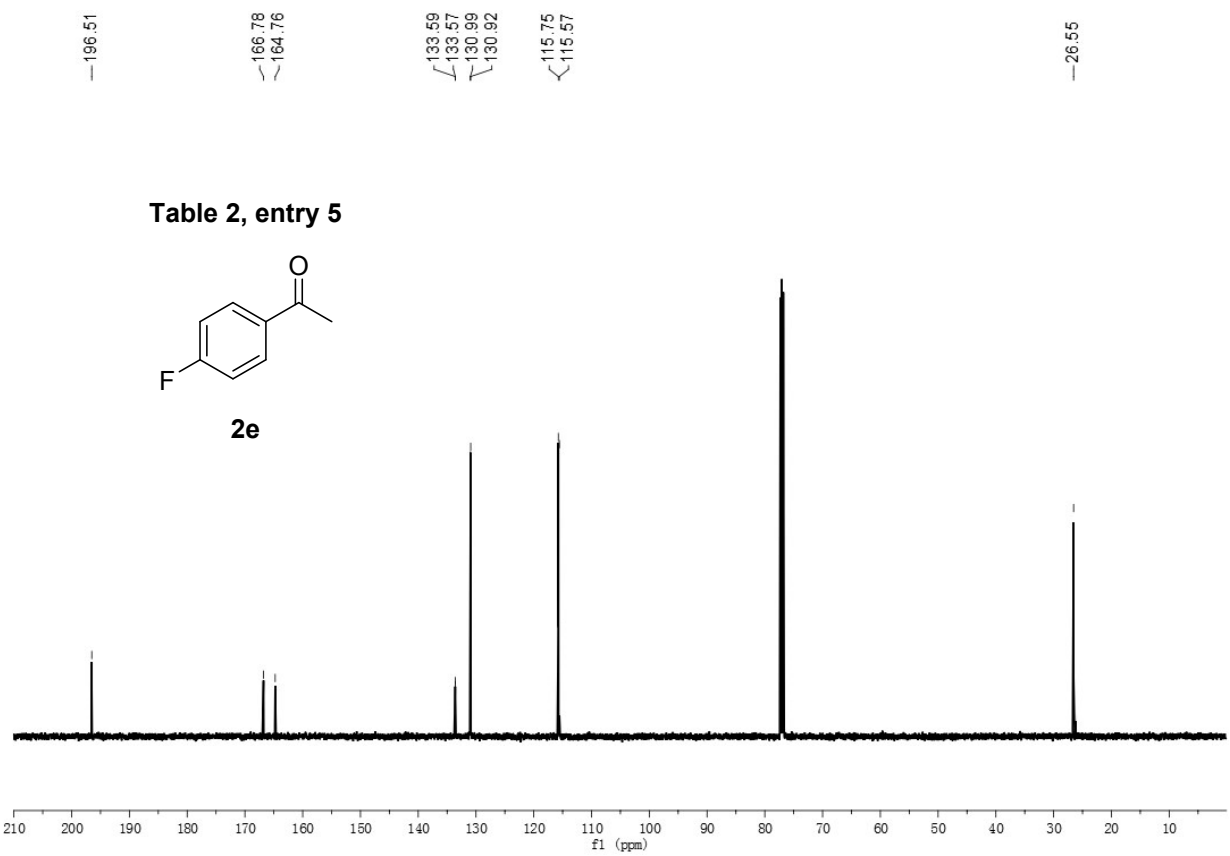

^{1}H NMR and ^{13}C NMR Spectrum of **2f**

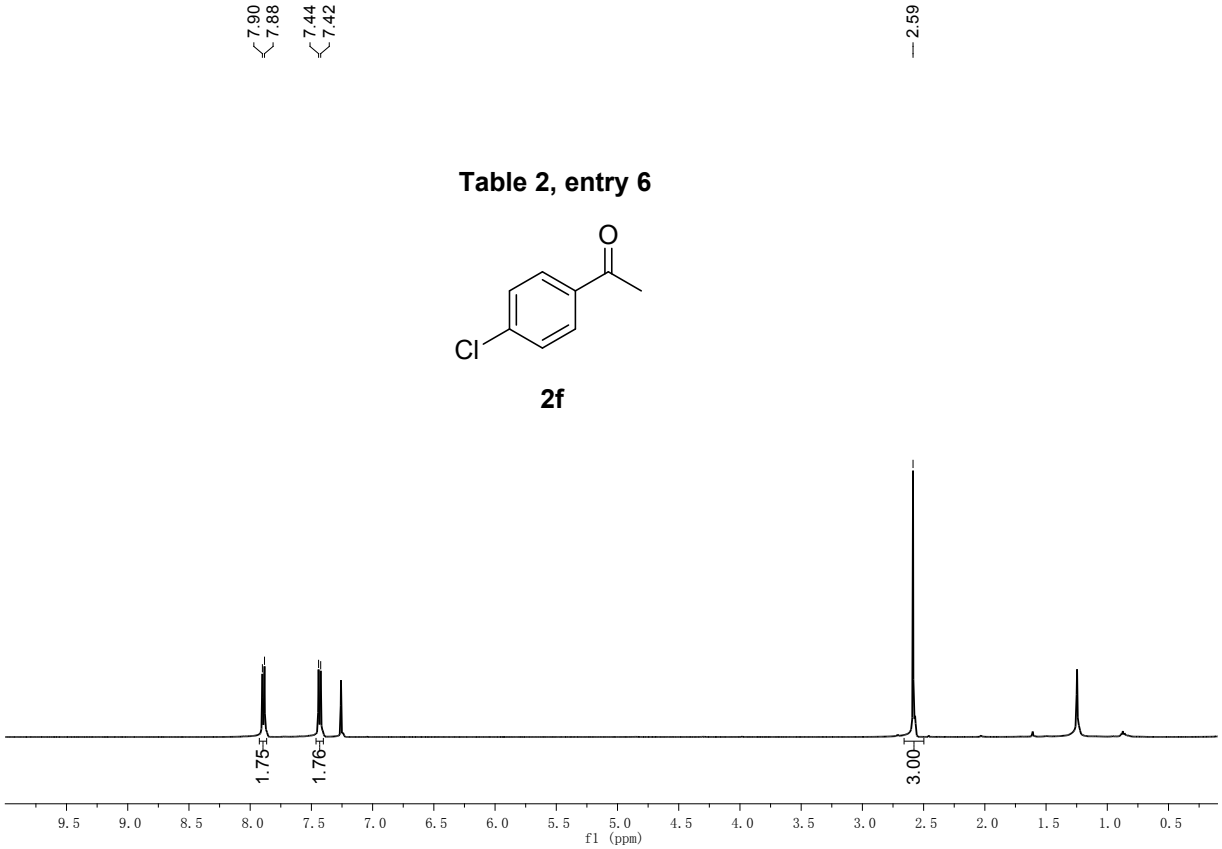

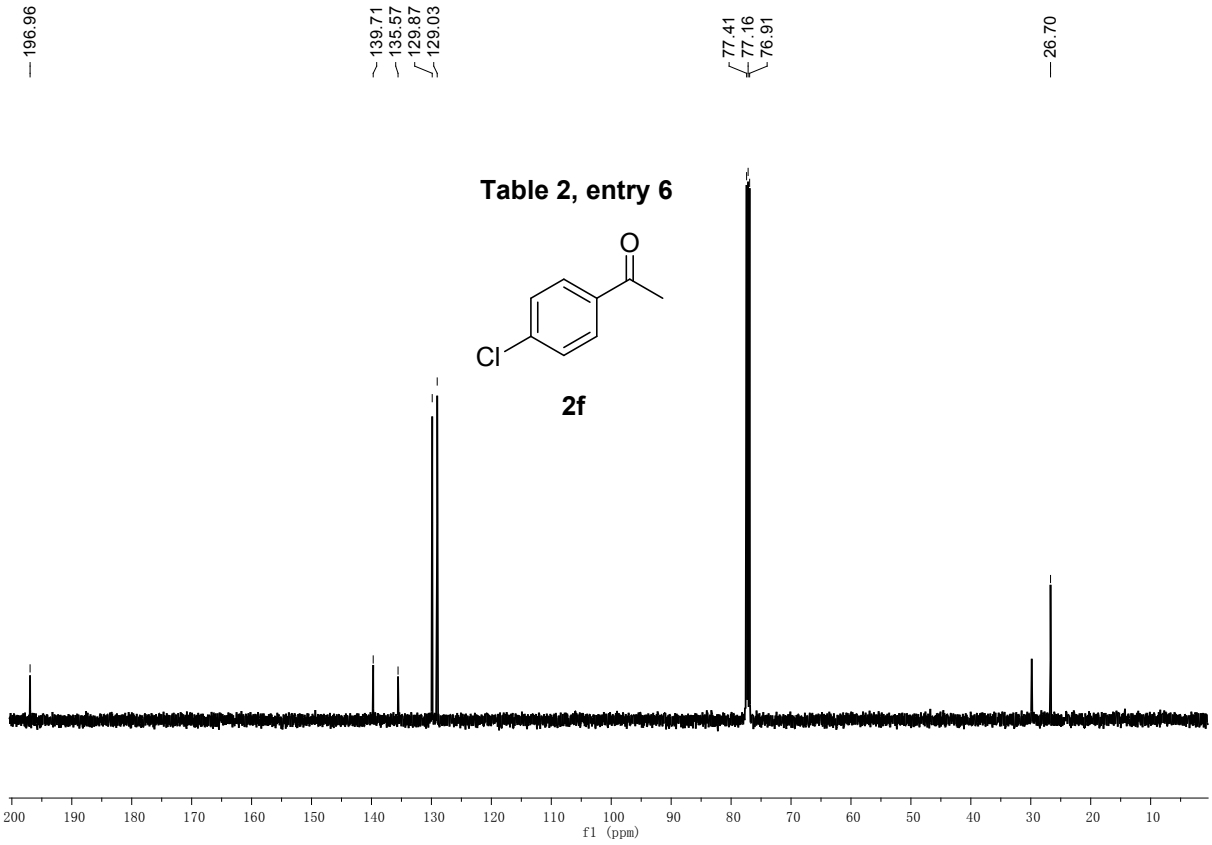

^{1}H NMR and ^{13}C NMR Spectrum of **2g**

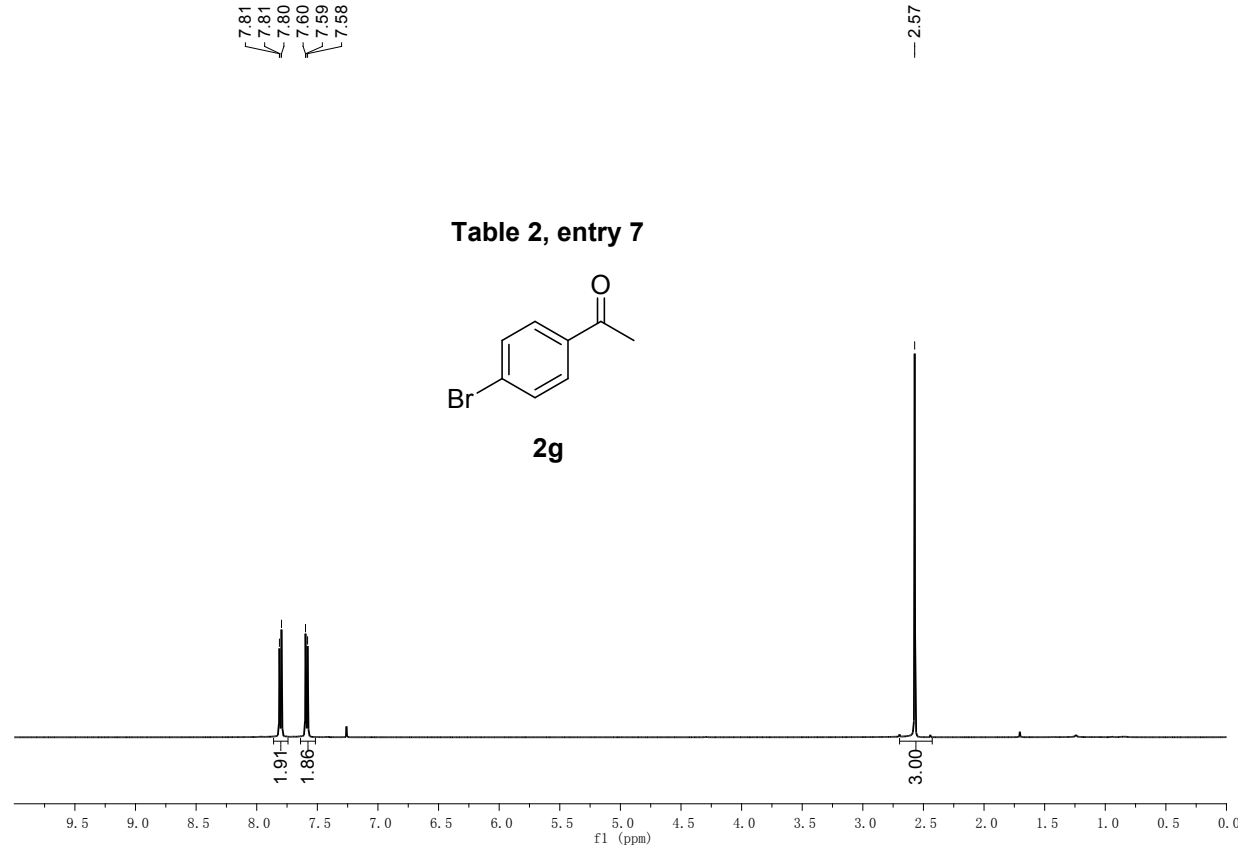

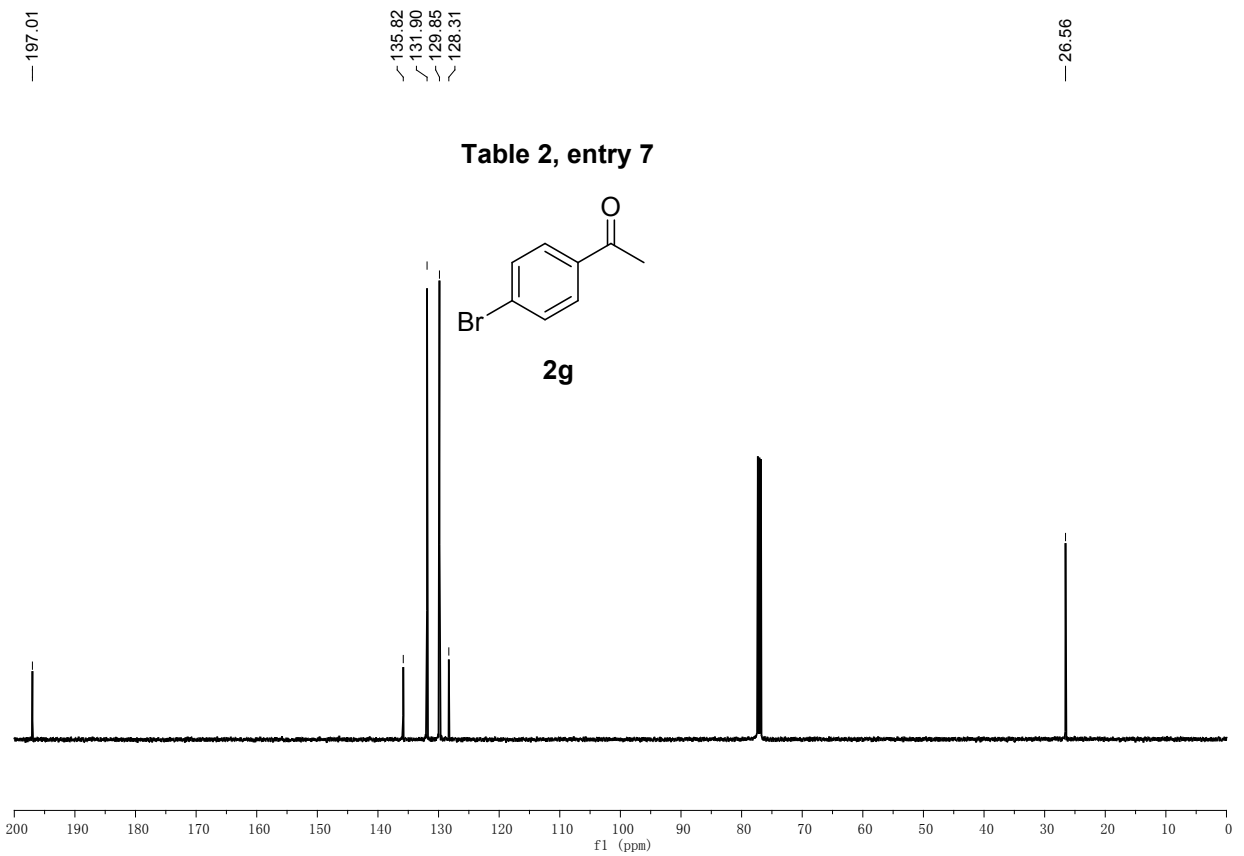

^{1}H NMR and ^{13}C NMR Spectrum of **2h**

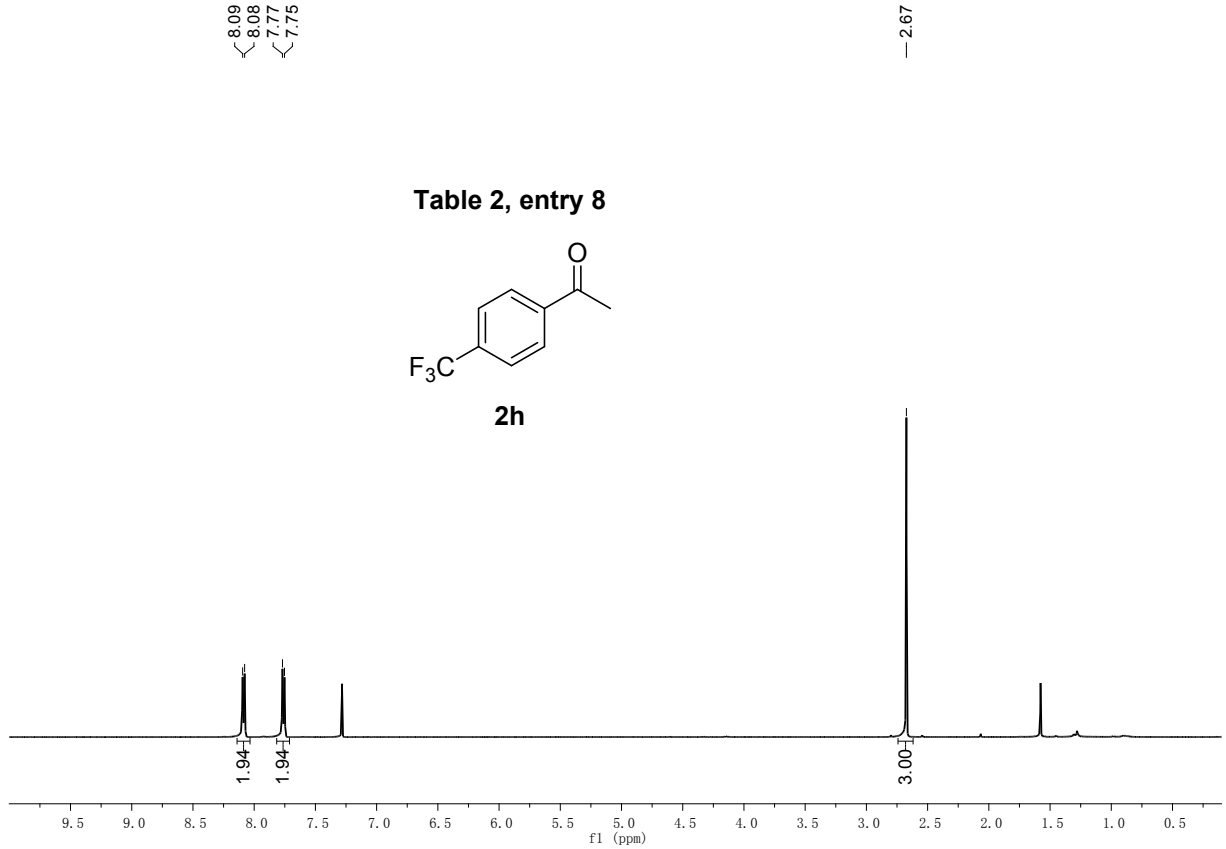

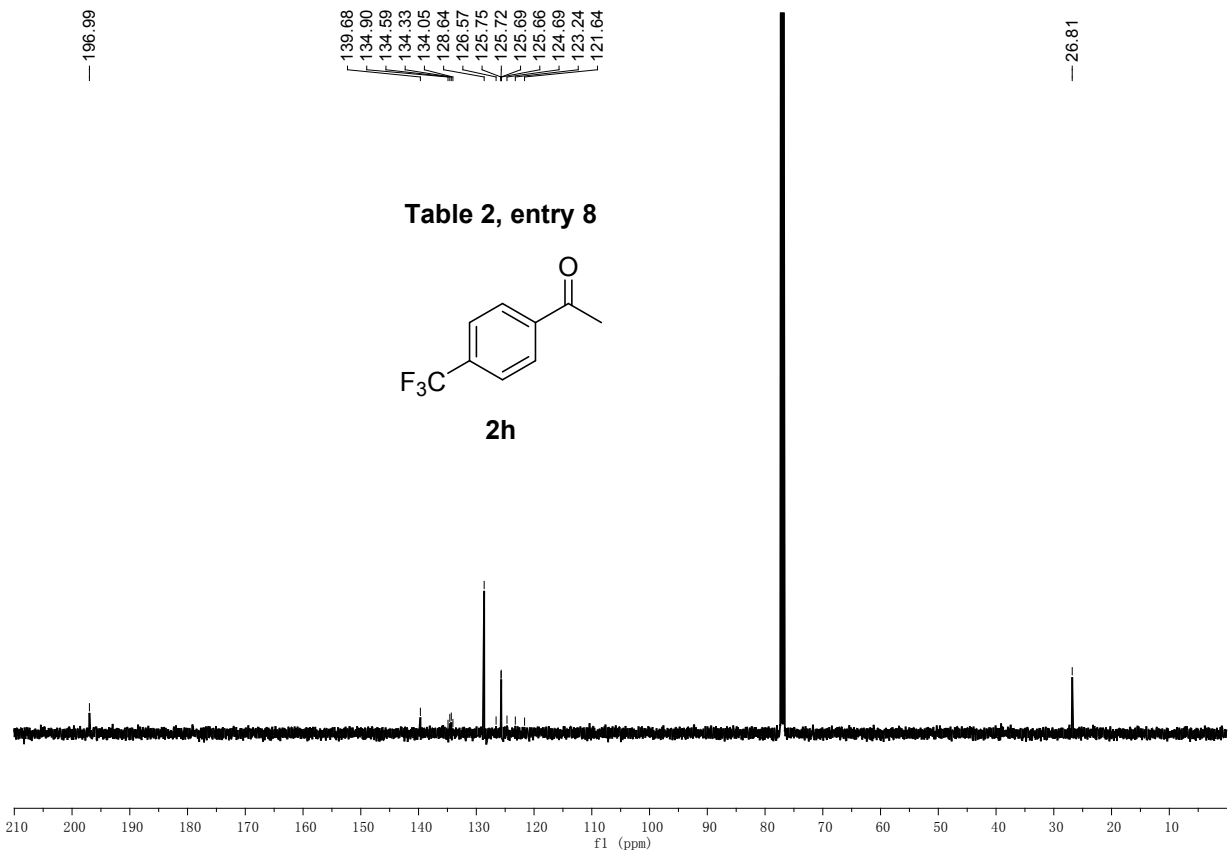

^{1}H NMR and ^{13}C NMR Spectrum of **2i**

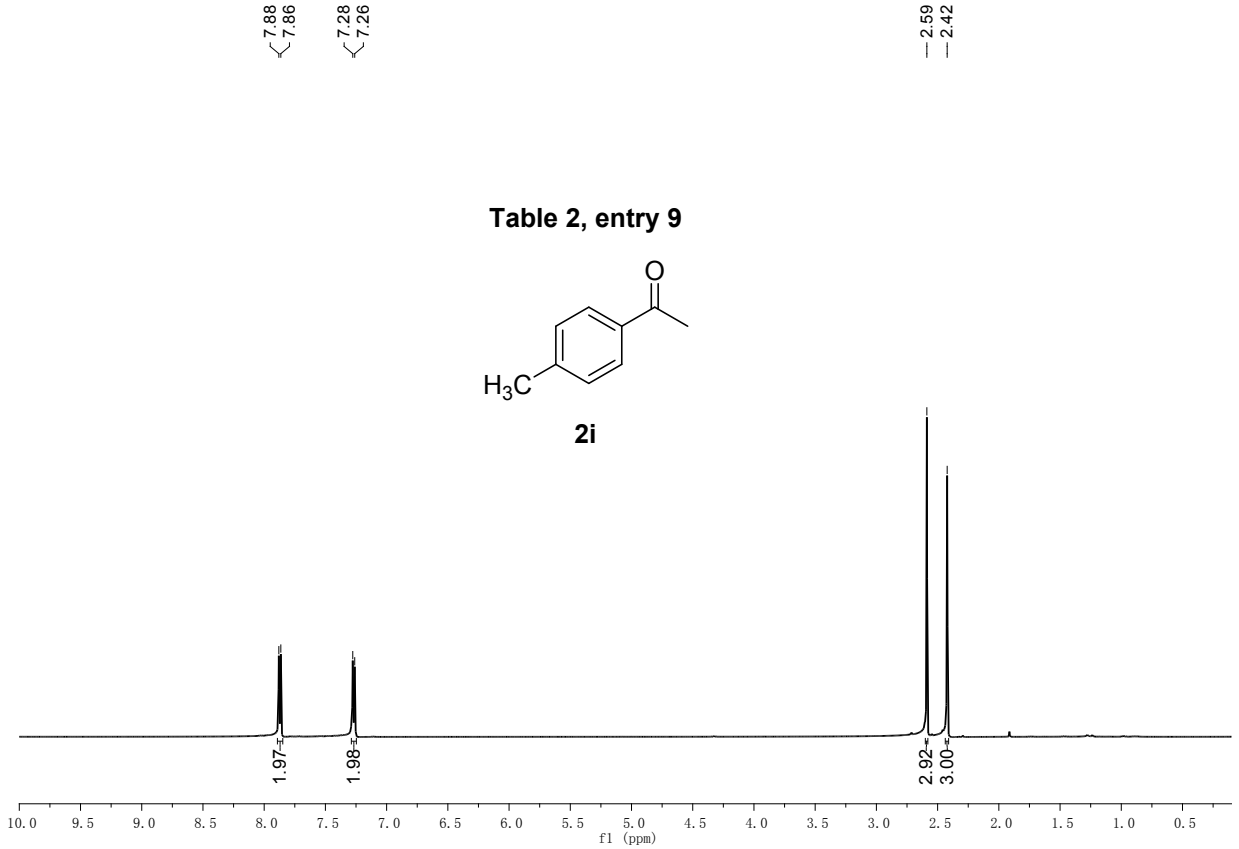

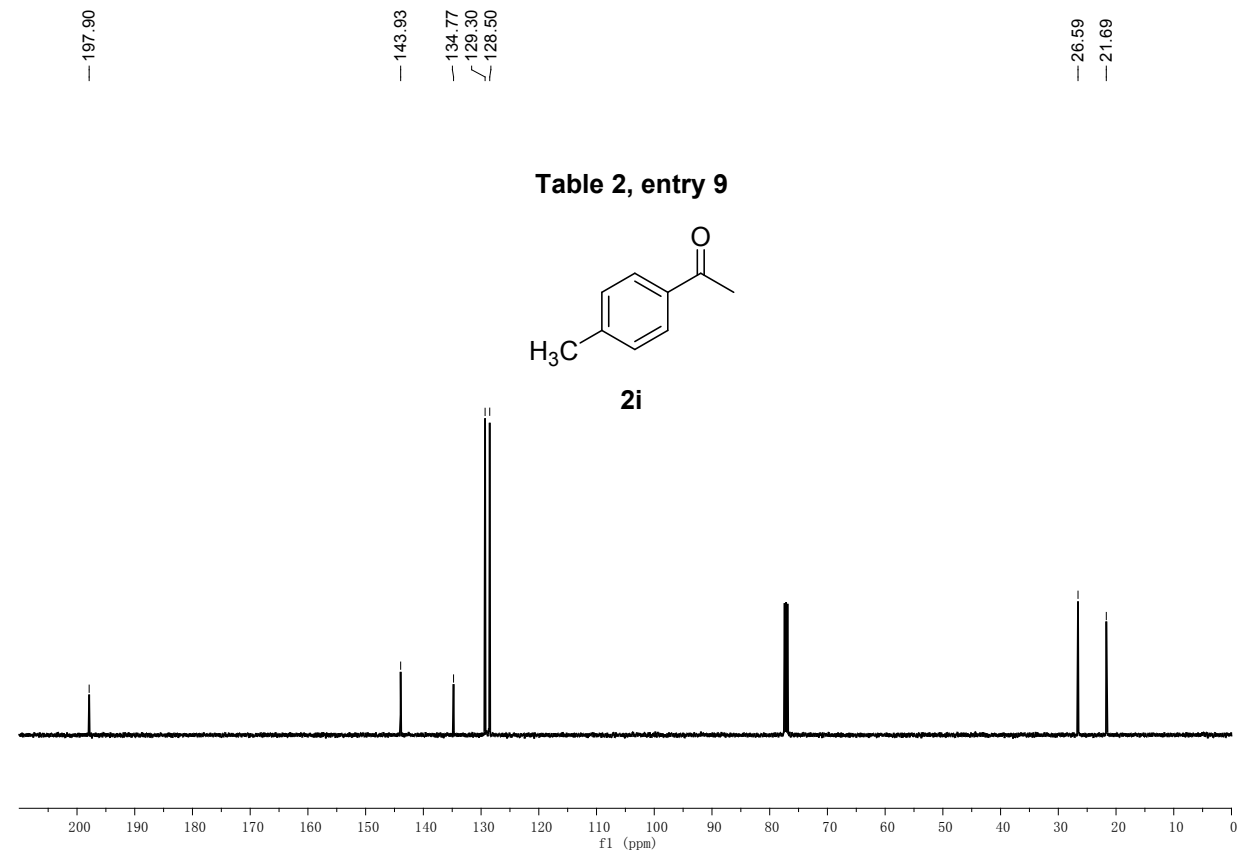

^{1}H NMR and ^{13}C NMR Spectrum of **2j**

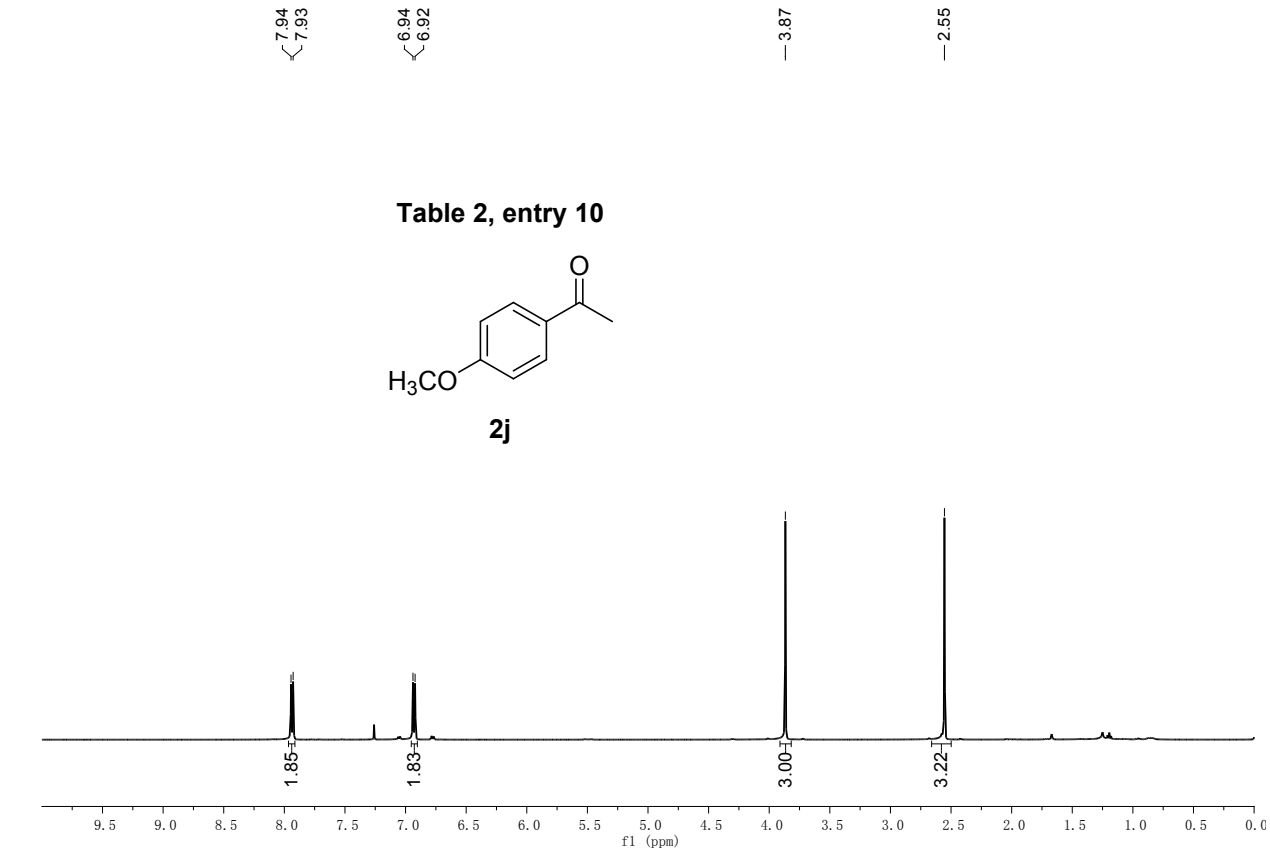

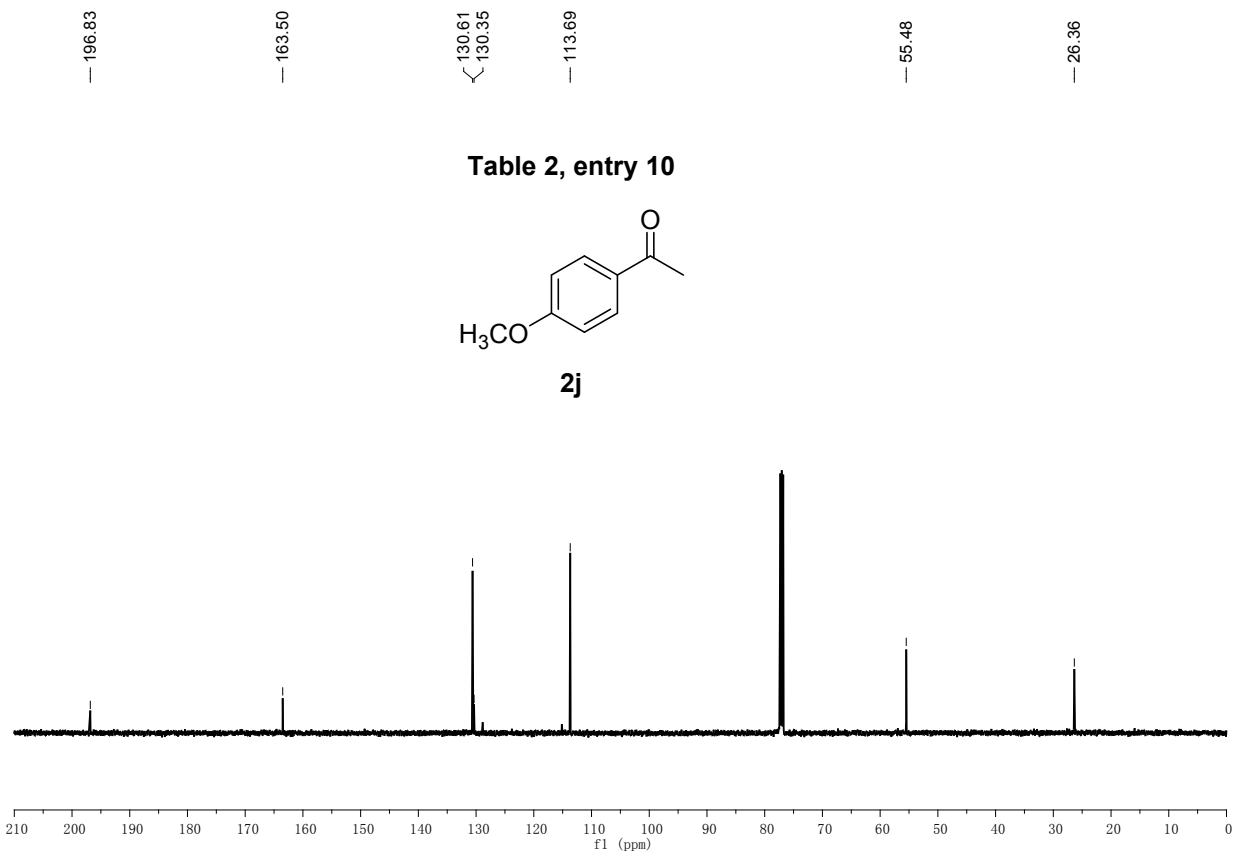

^{1}H NMR and ^{13}C NMR Spectrum of **2k**

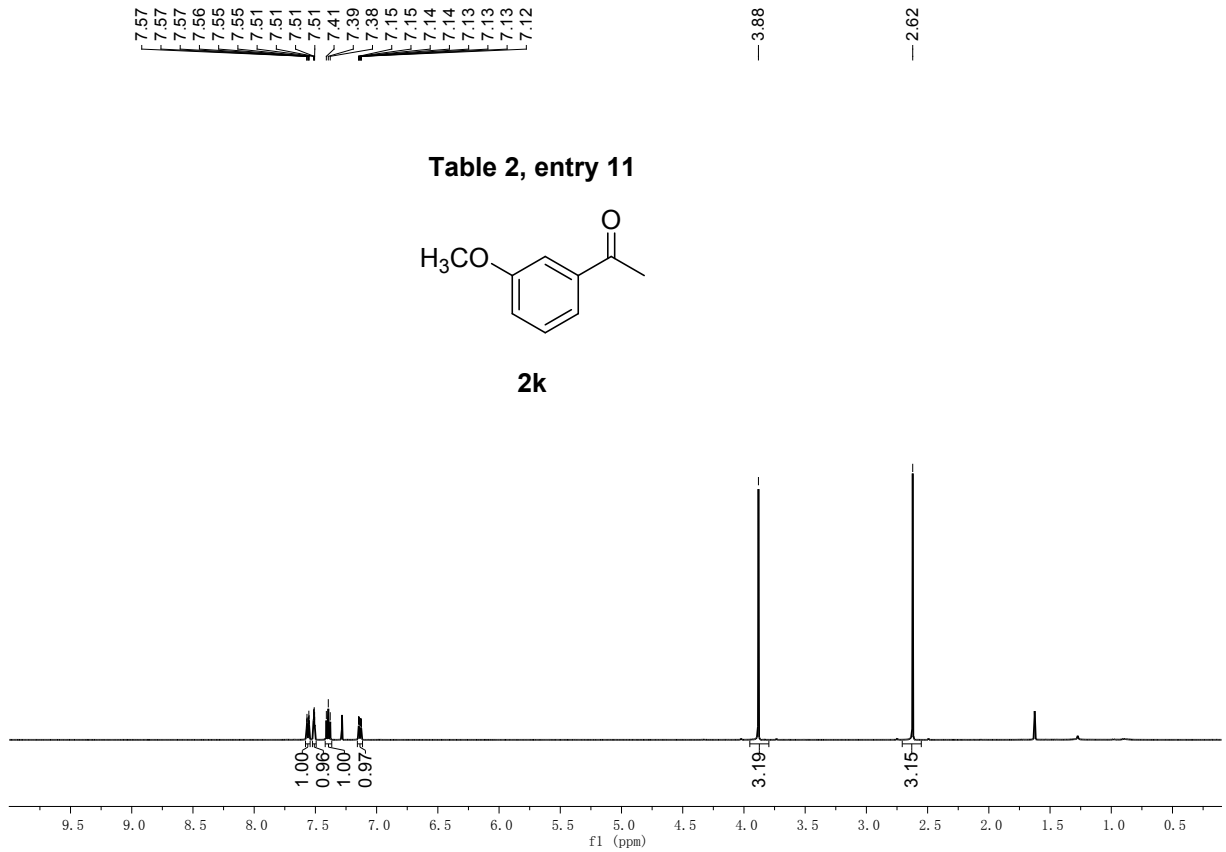

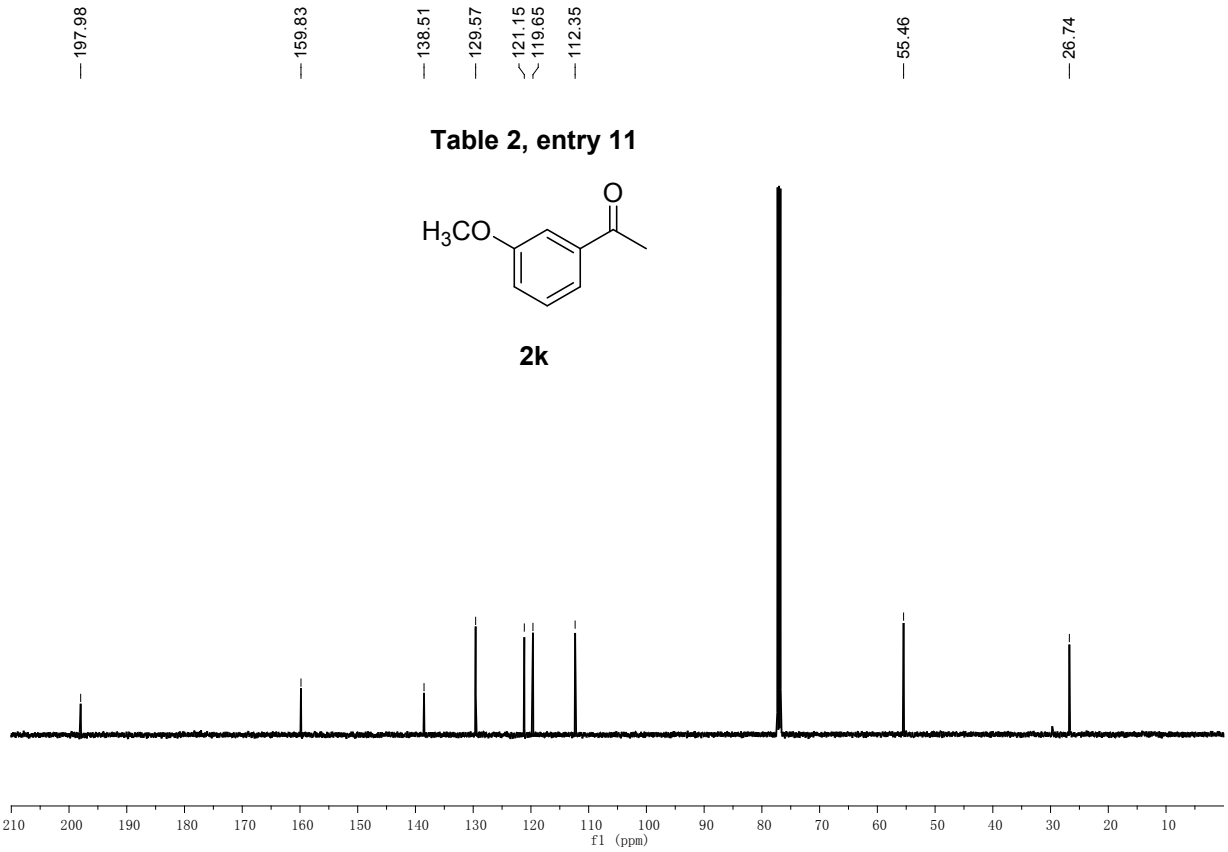

^{1}H NMR and ^{13}C NMR Spectrum of **2l**

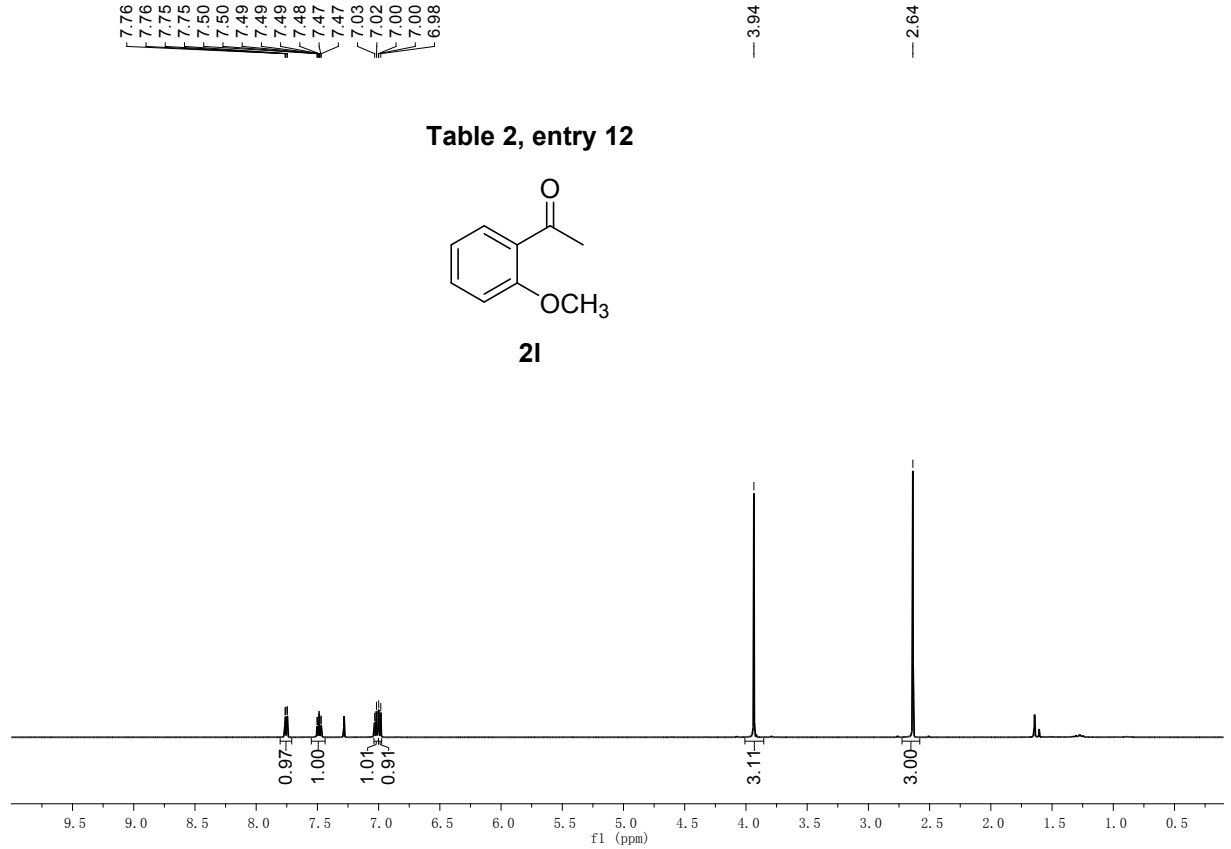

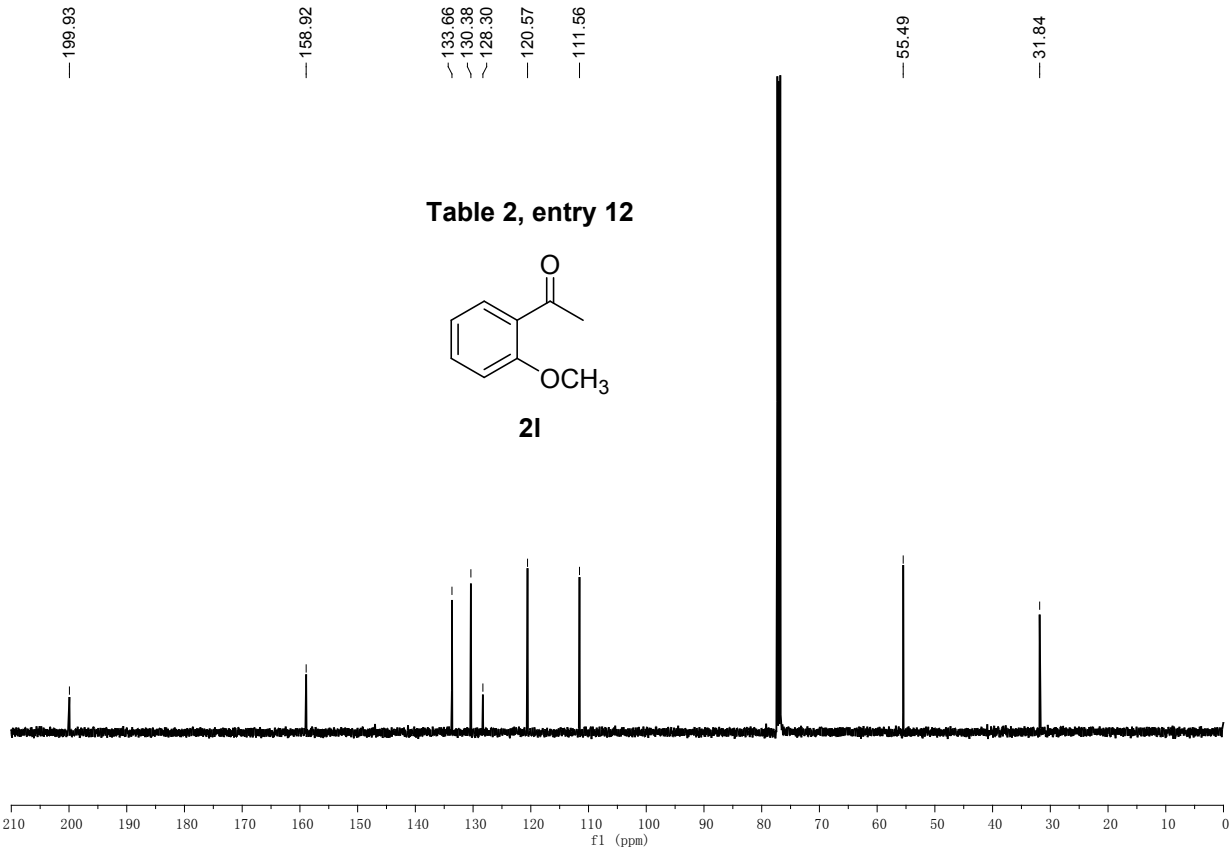

^{1}H NMR and ^{13}C NMR Spectrum of **2m**

Table 2, entry 13

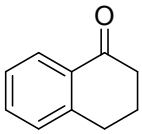

2m

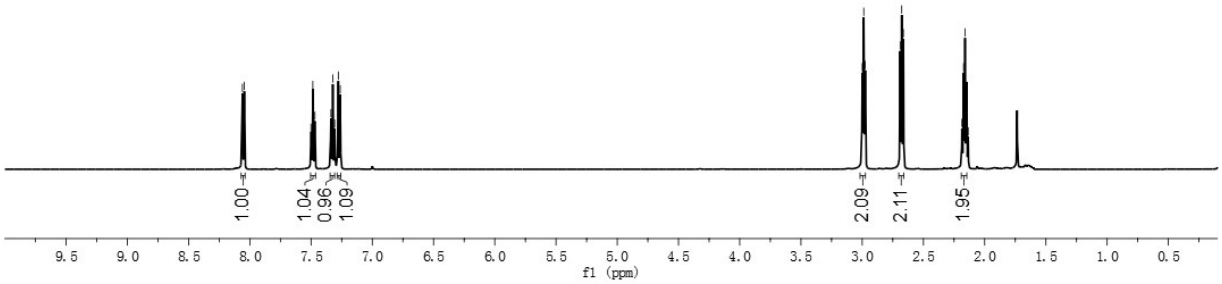

Table 2, entry 13

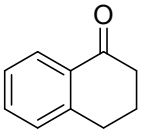

2m

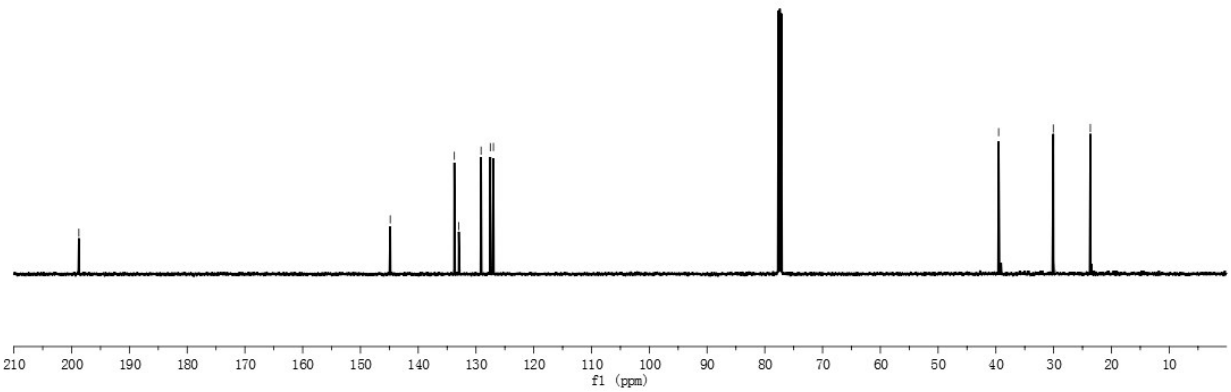

^{1}H NMR and ^{13}C NMR Spectrum of **2n**

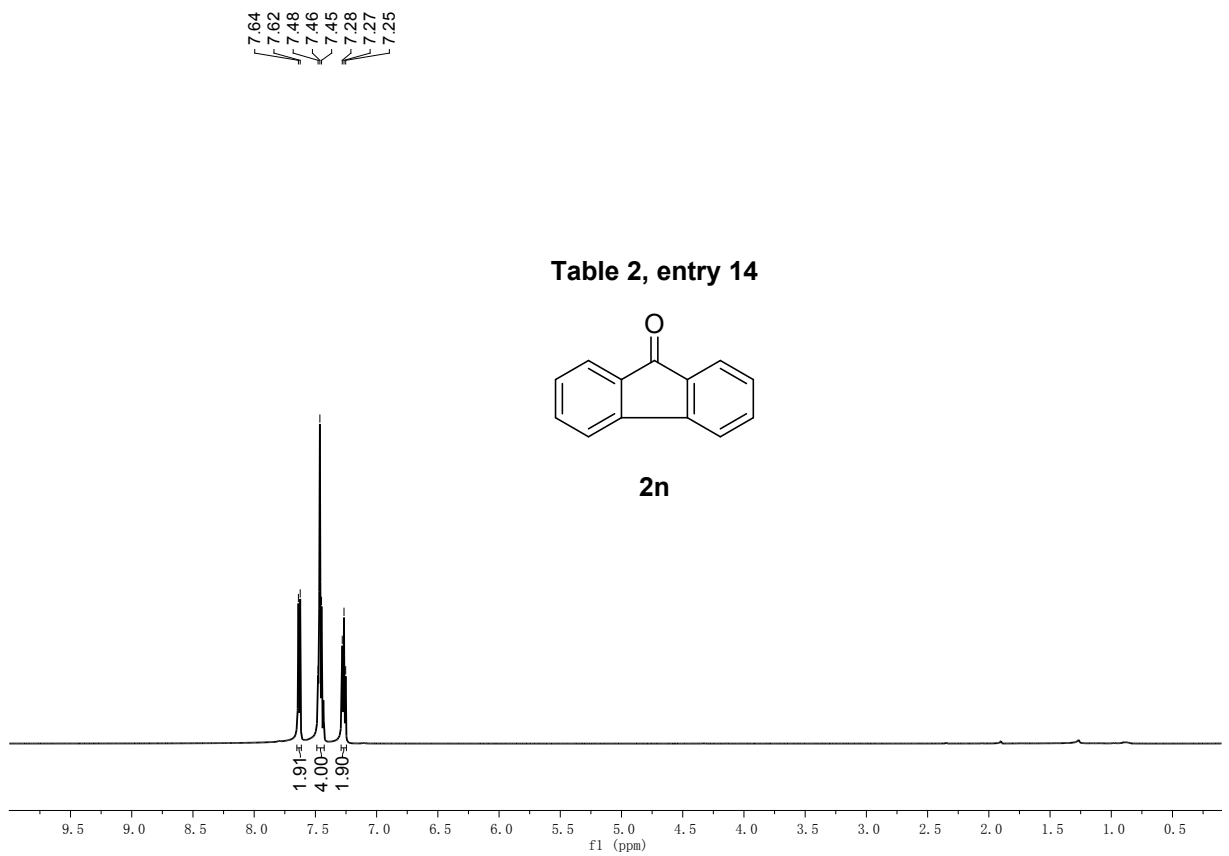

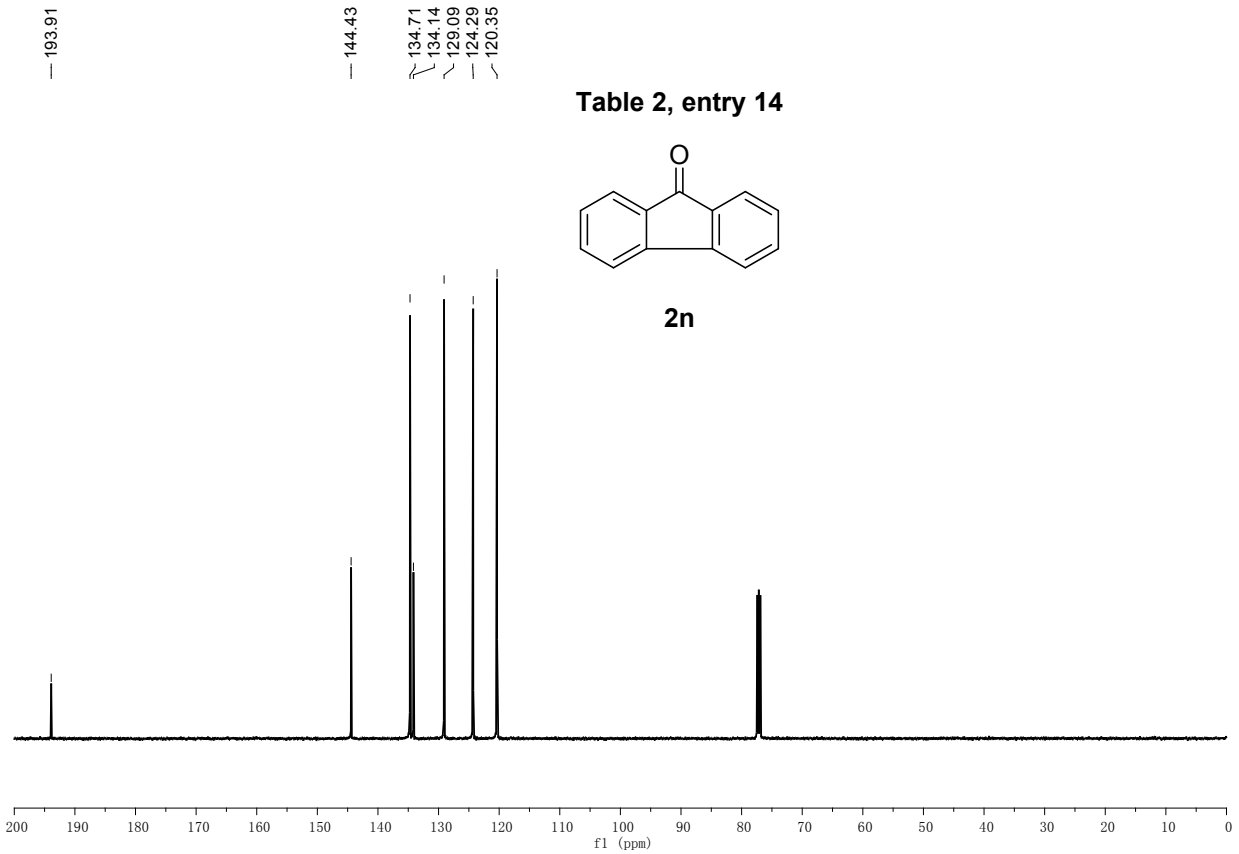

^{1}H NMR and ^{13}C NMR Spectrum of **2o**

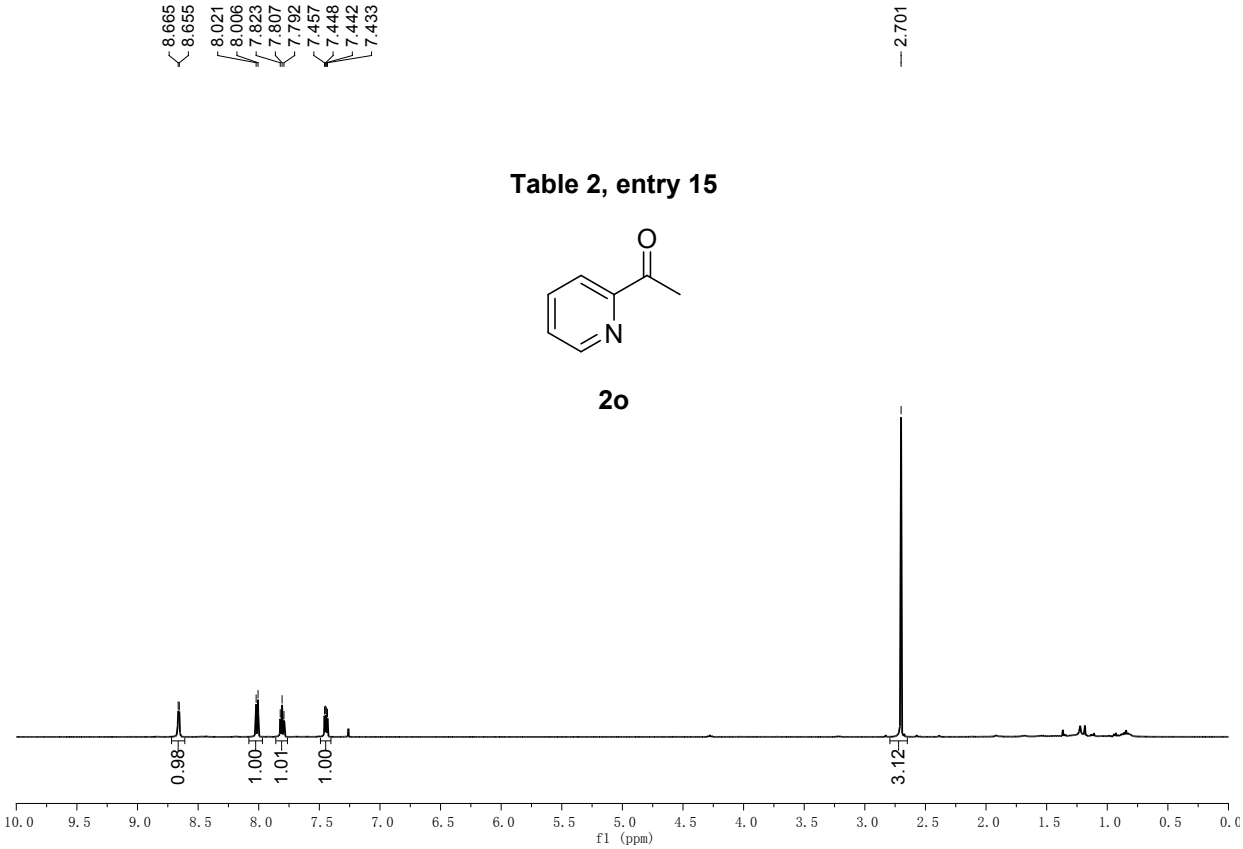

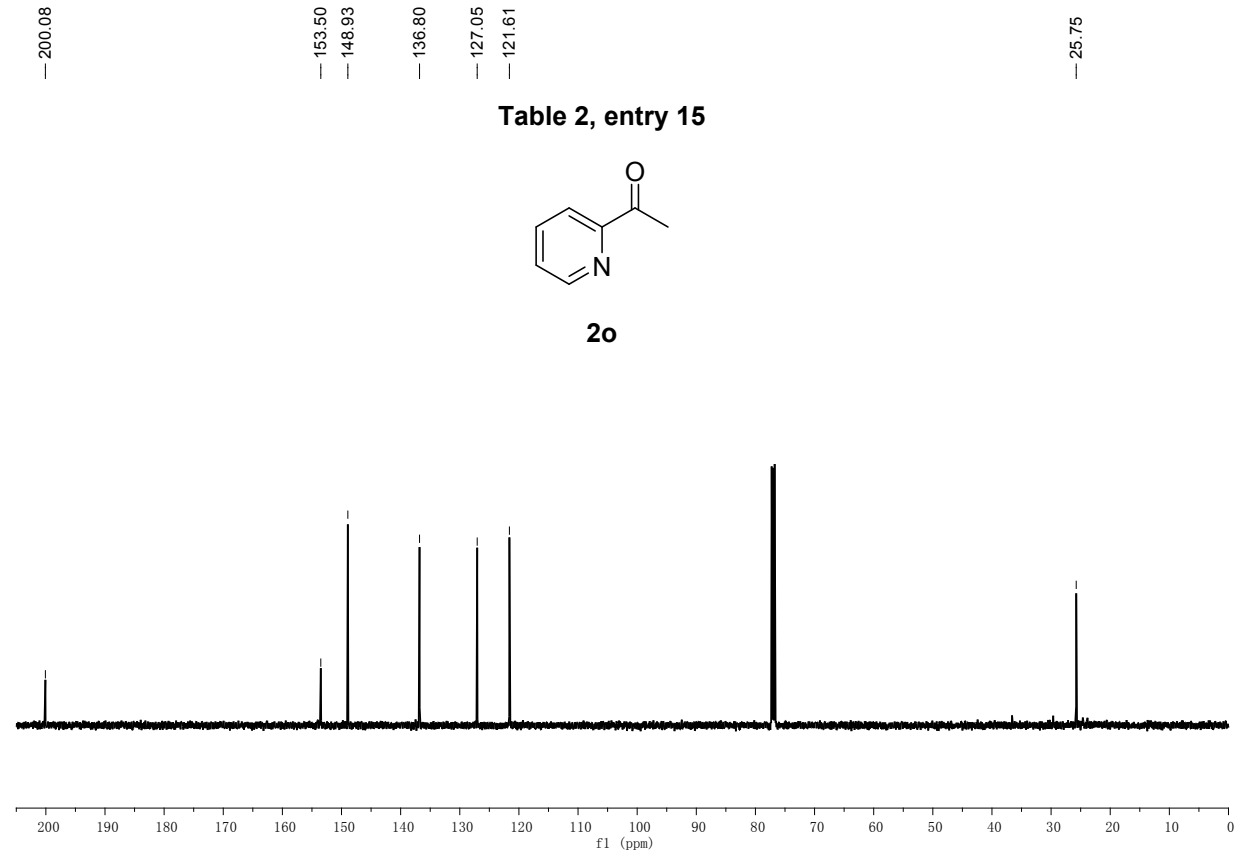

^{1}H NMR and ^{13}C NMR Spectrum of **2p**

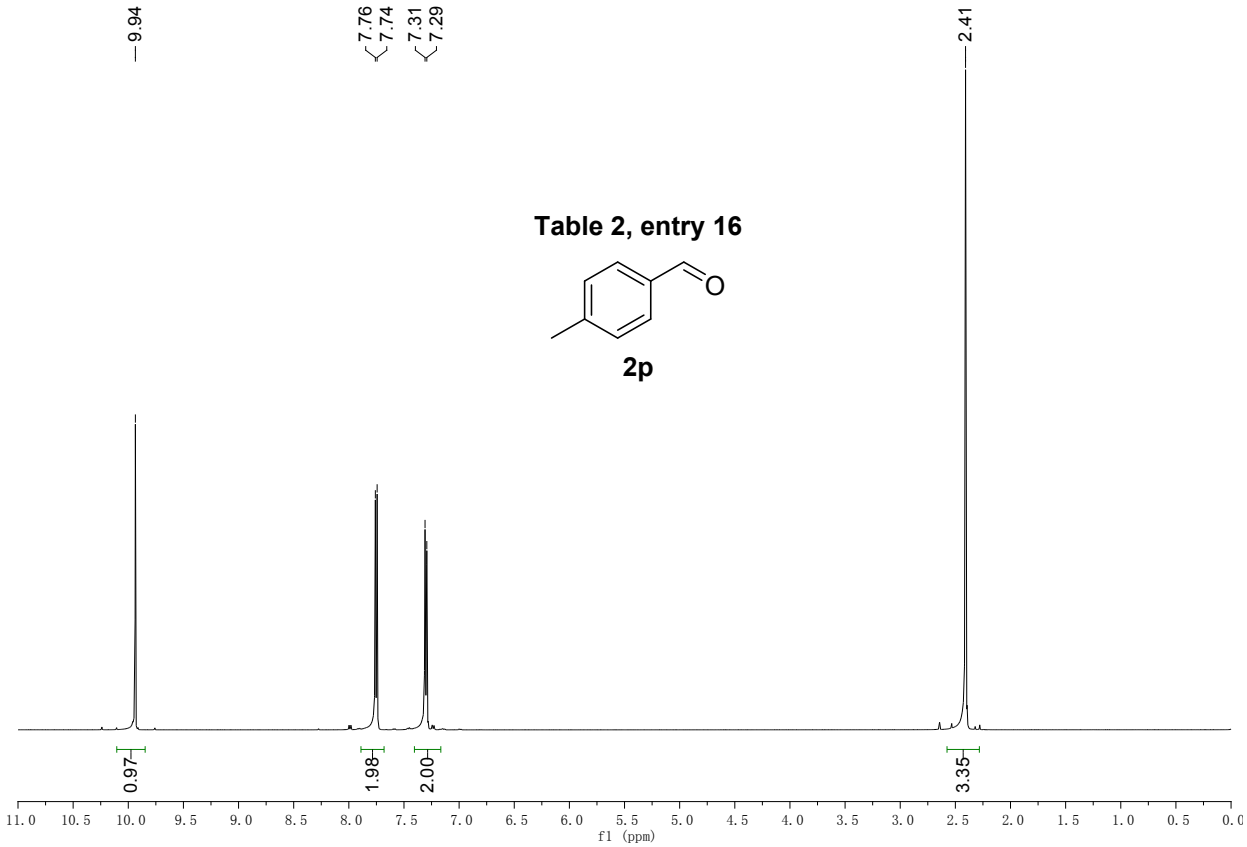

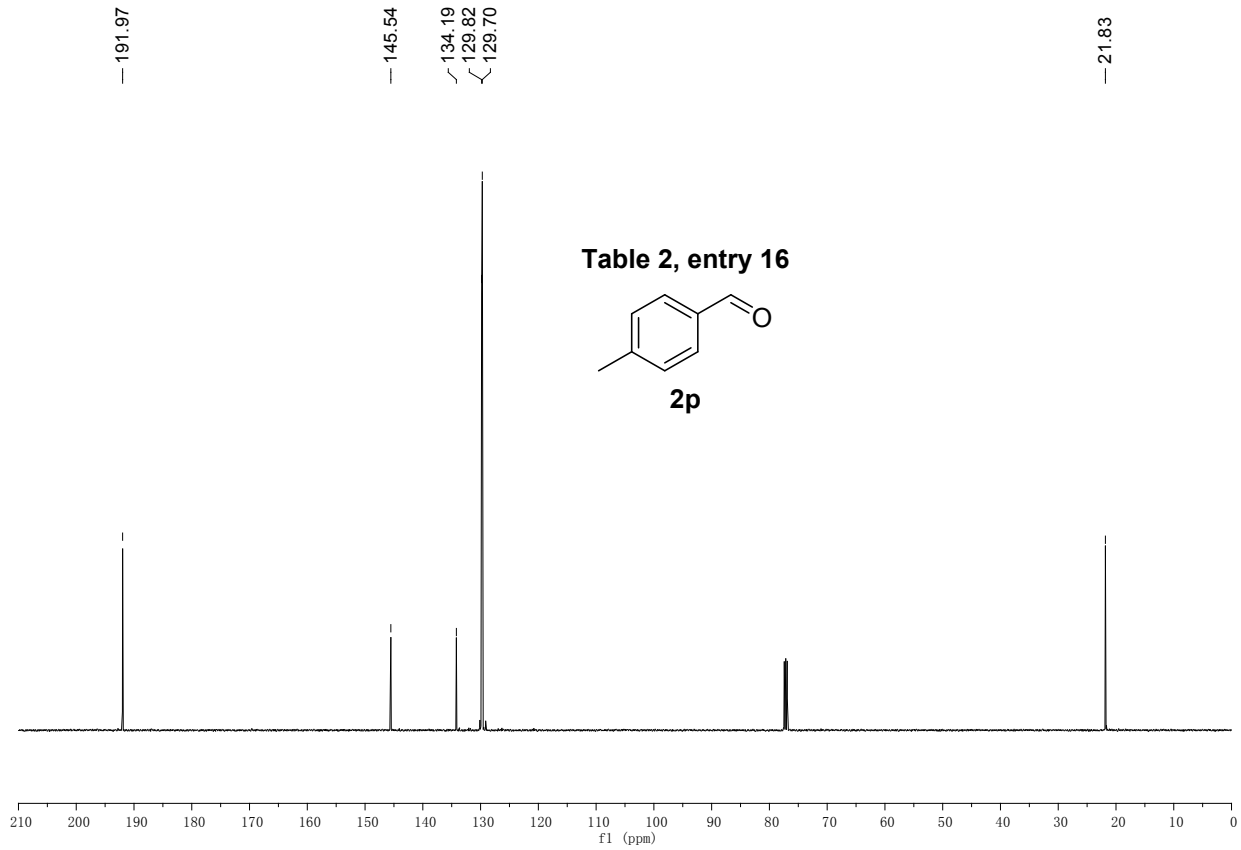

^{1}H NMR and ^{13}C NMR Spectrum of **2q**

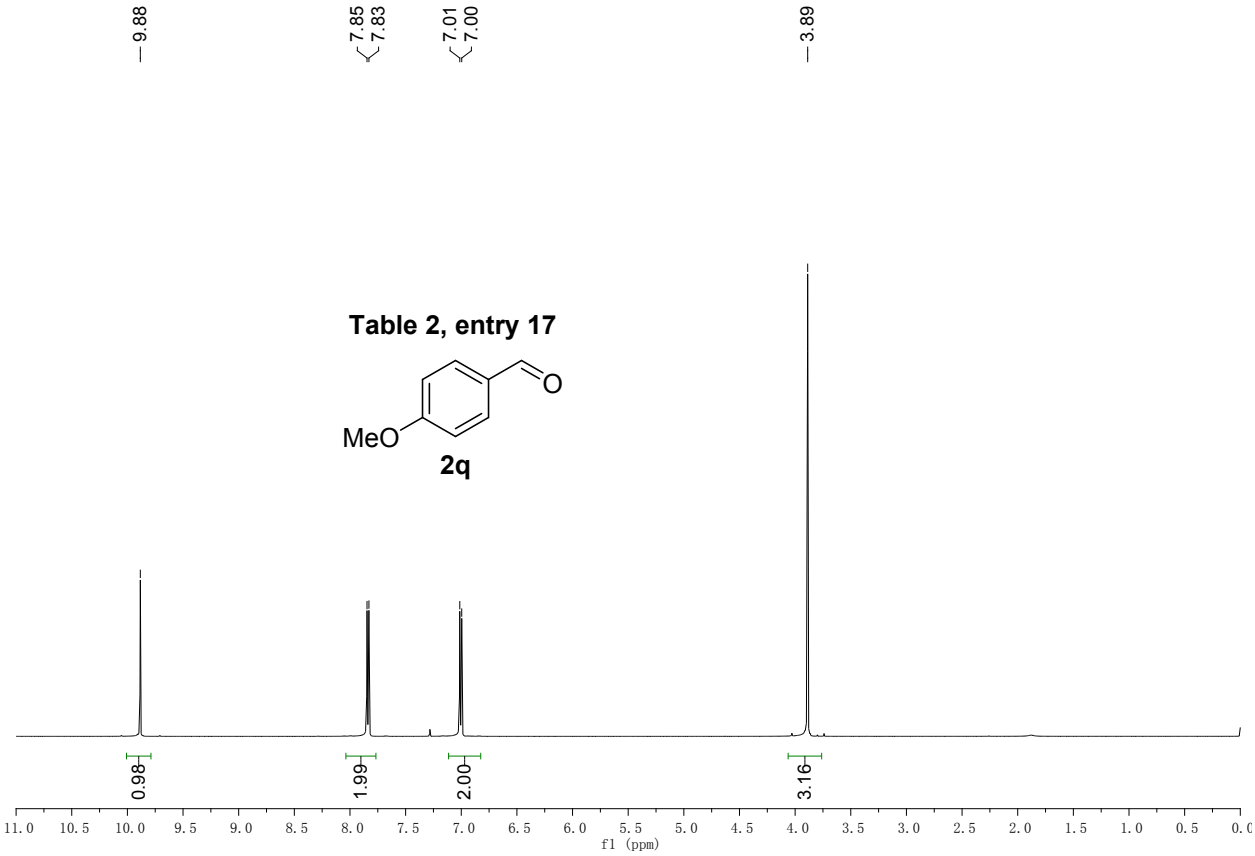

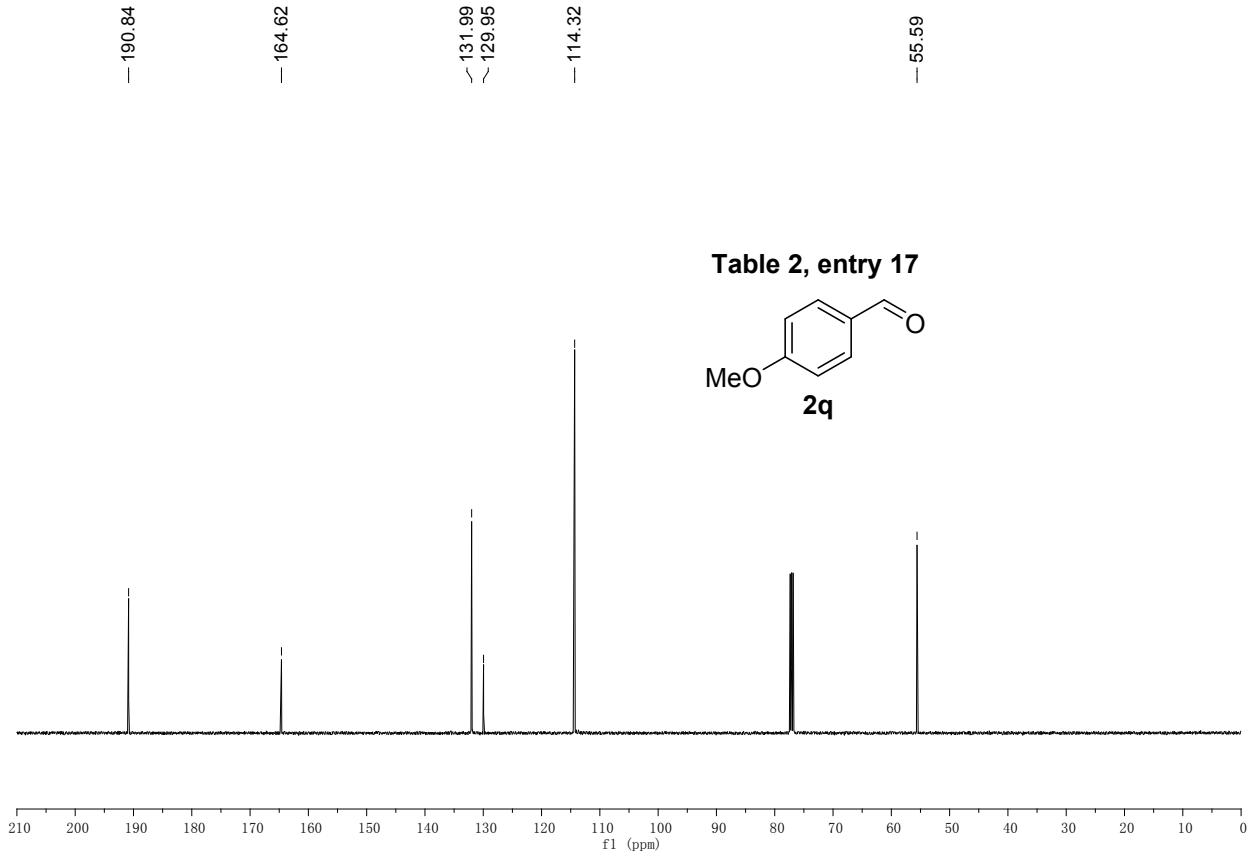

^{1}H NMR and ^{13}C NMR Spectrum of **2r**

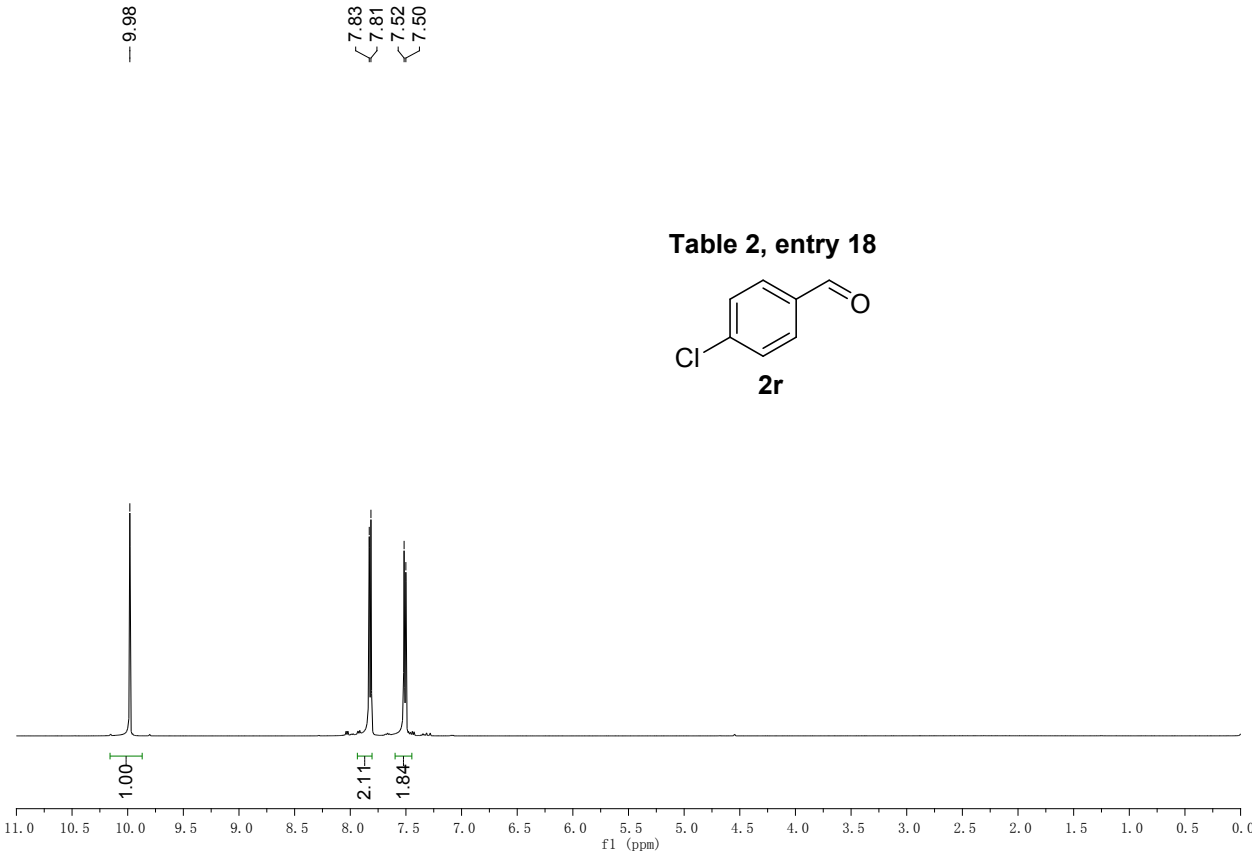

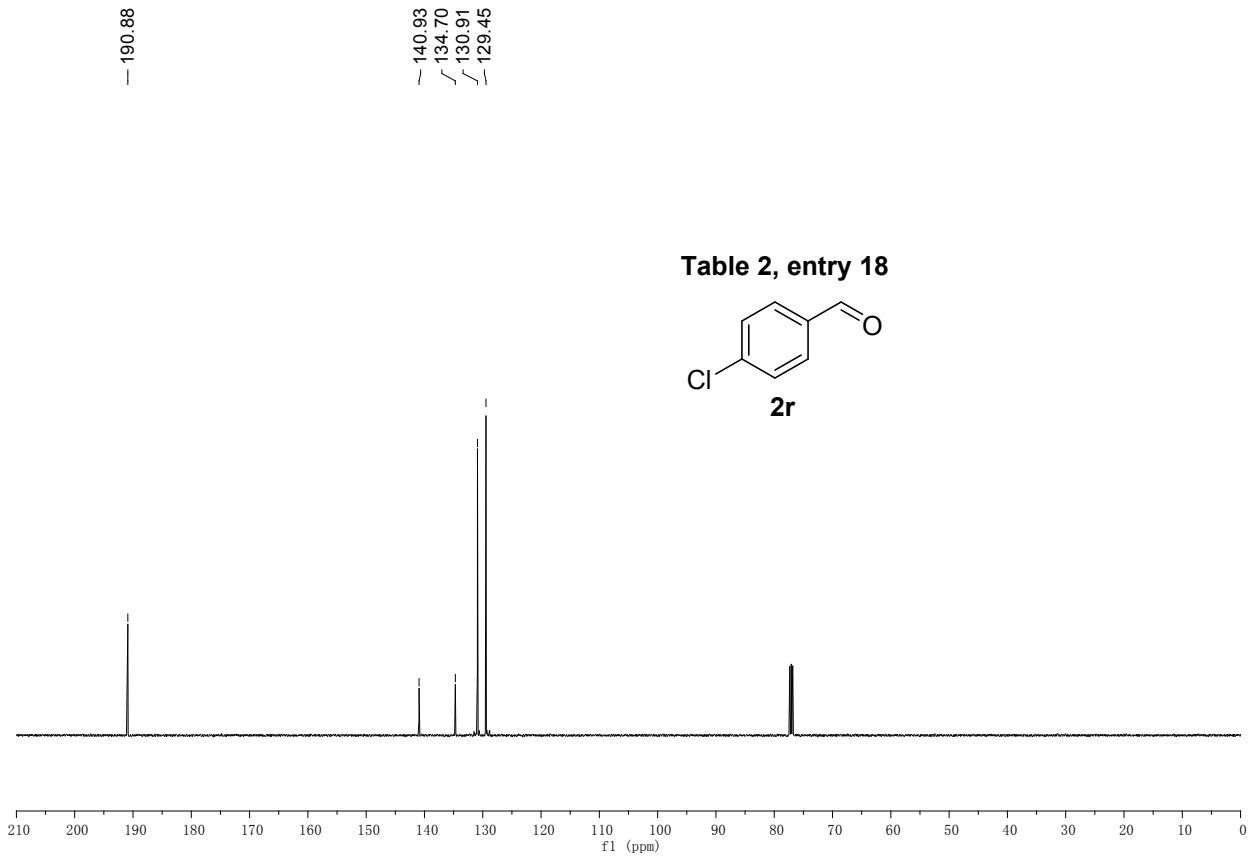

^{1}H NMR and ^{13}C NMR Spectrum of **2s**

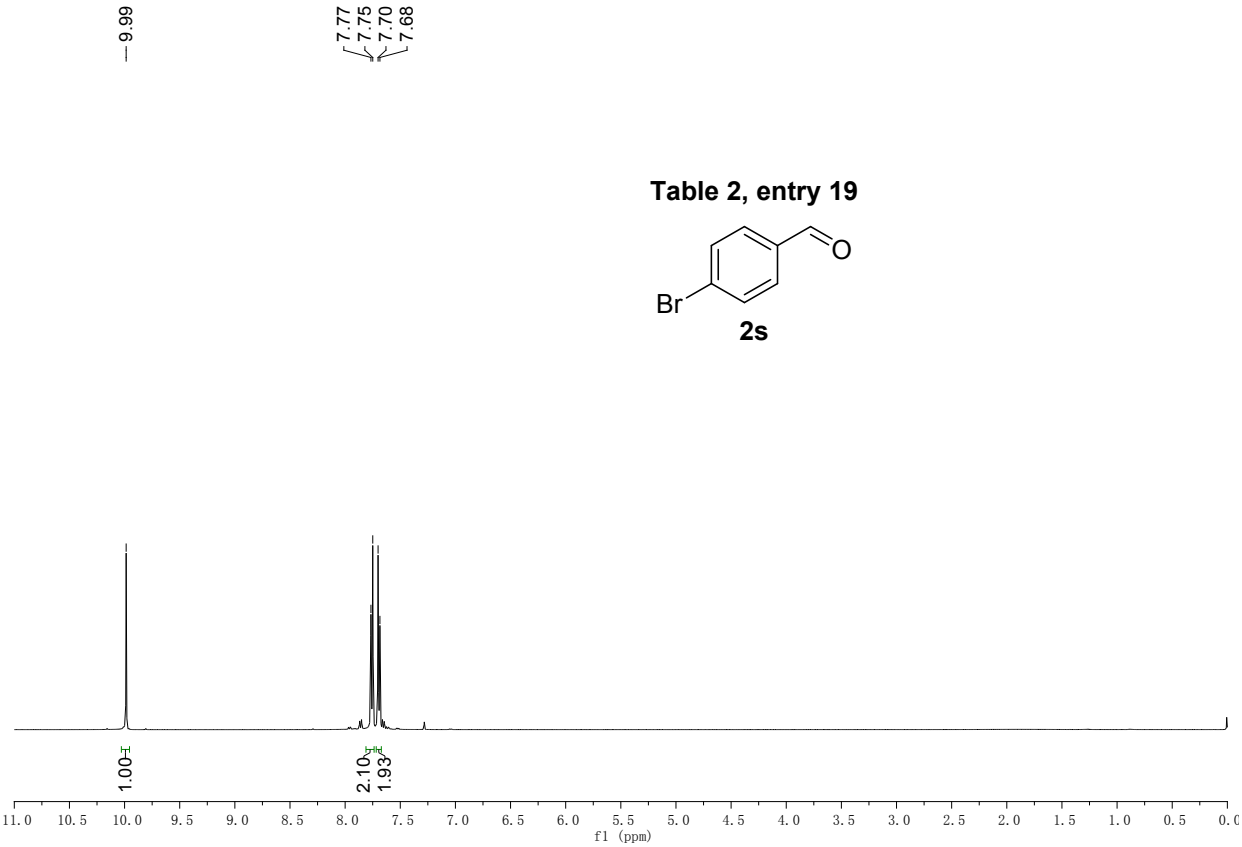

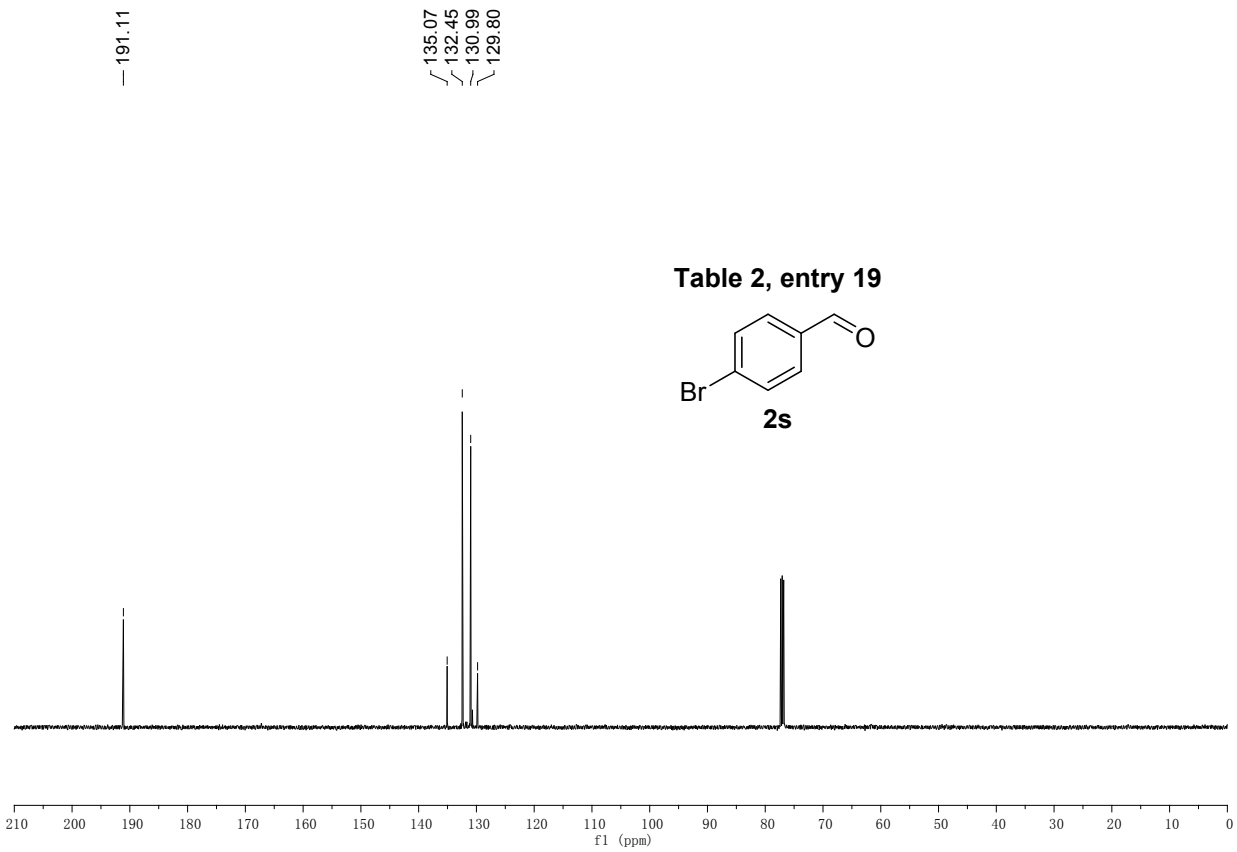

^{1}H NMR and ^{13}C NMR Spectrum of **2t**

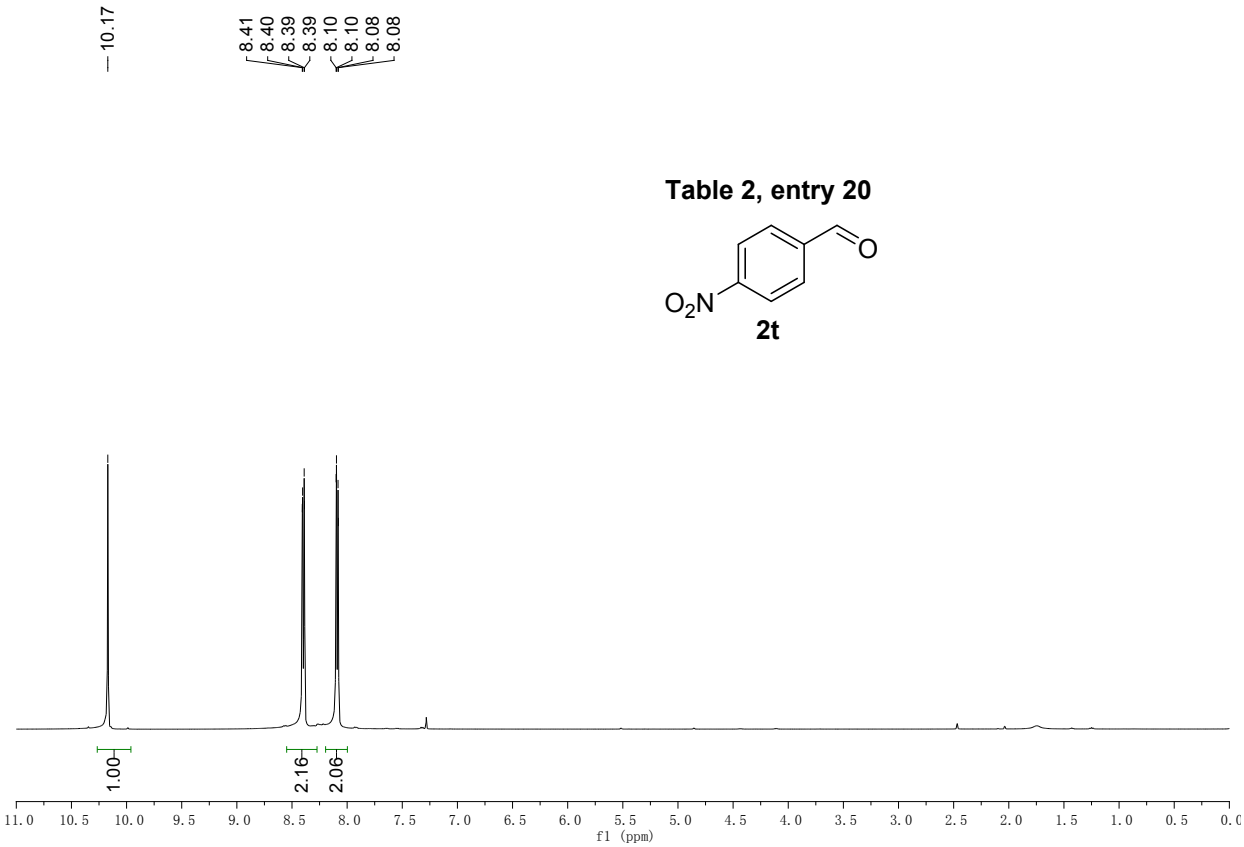

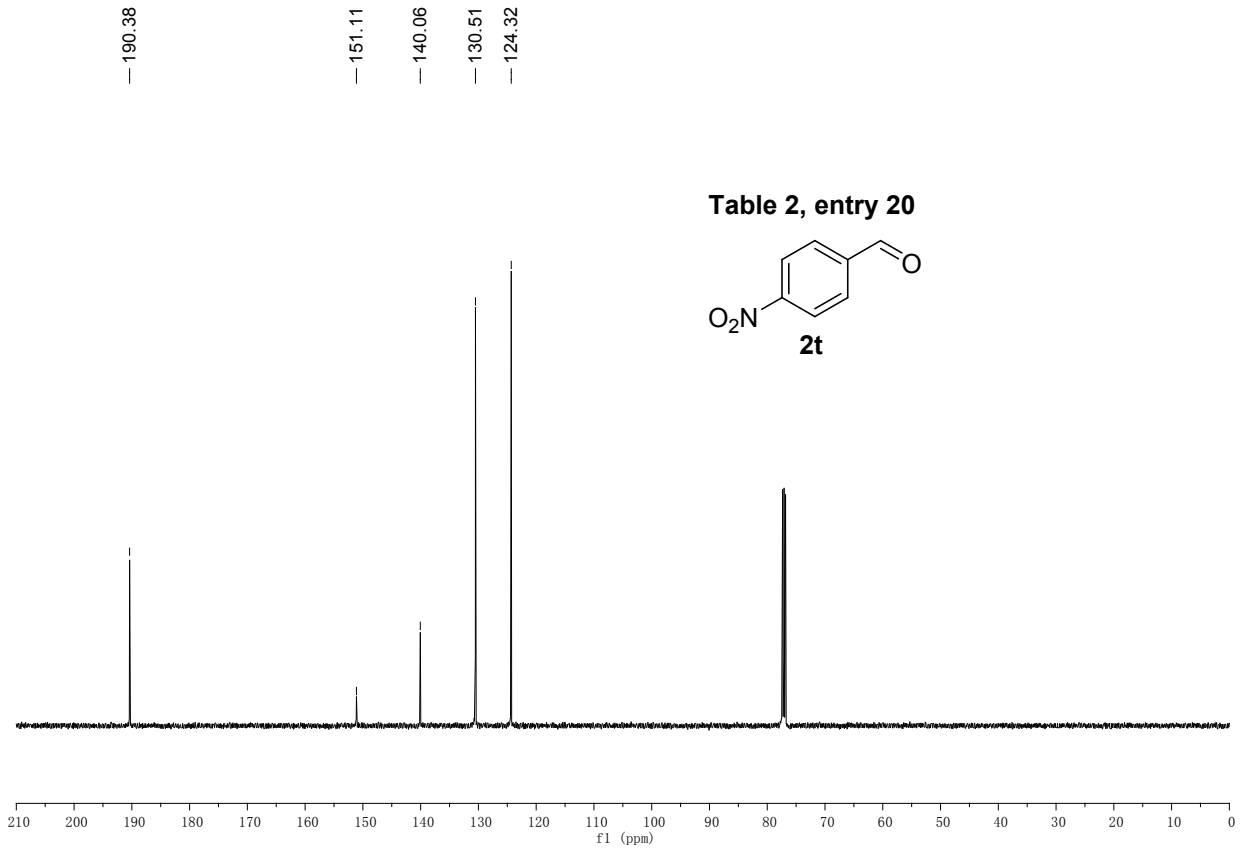

^{1}H NMR and ^{13}C NMR Spectrum of **2u**

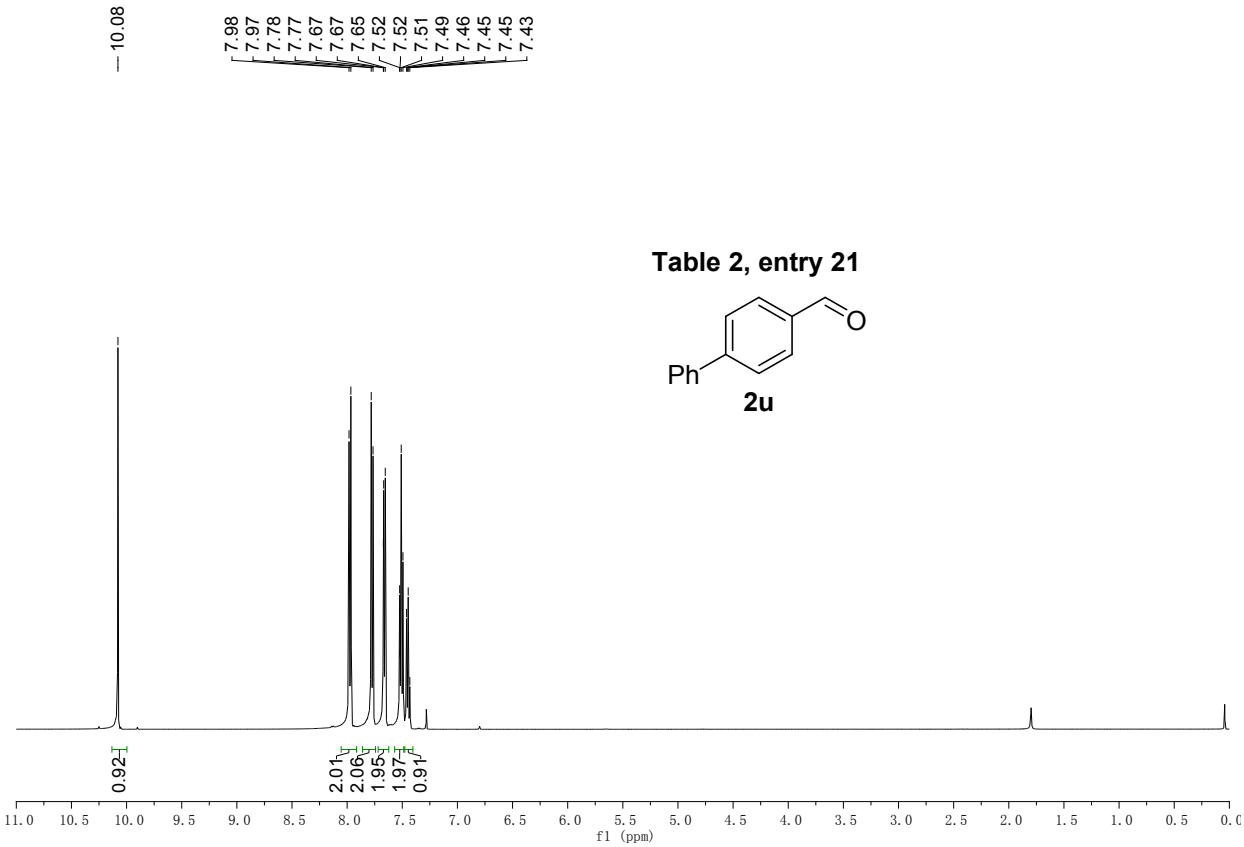

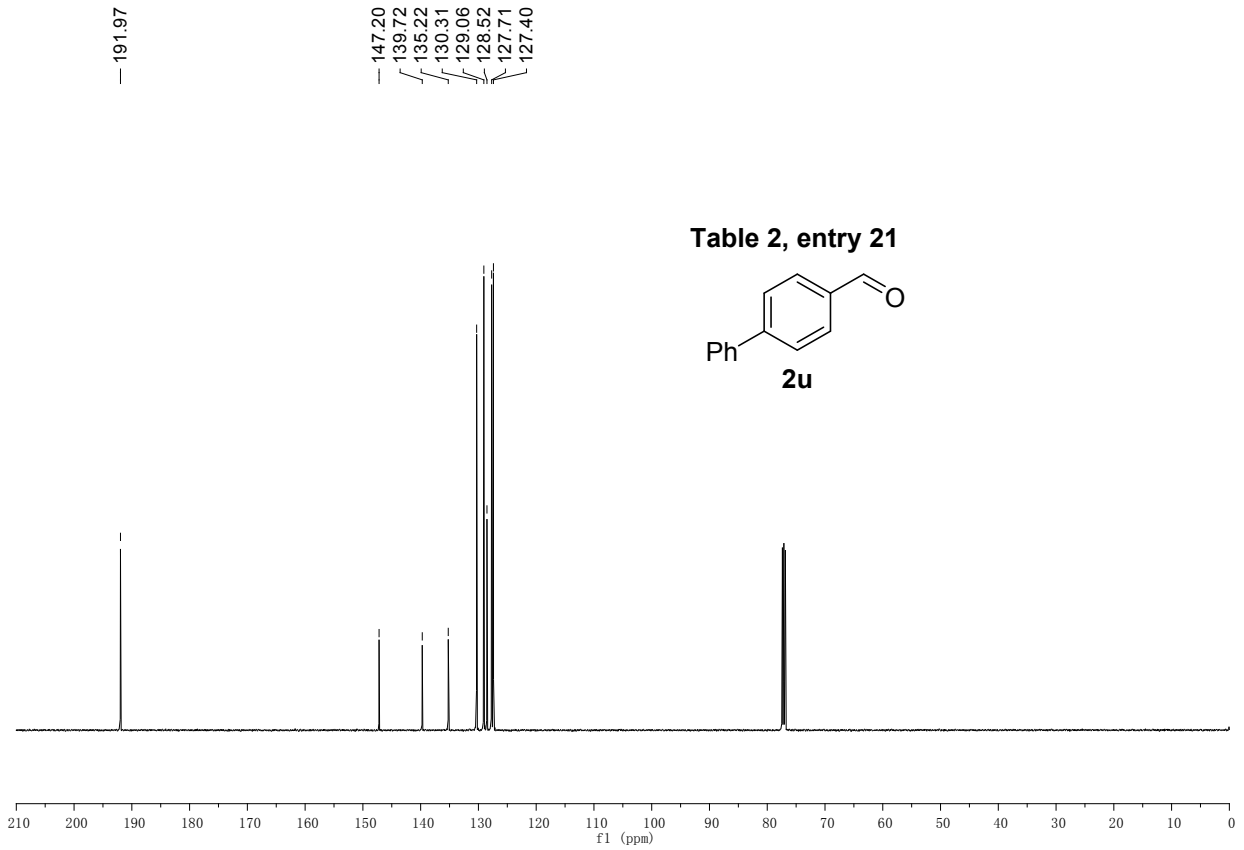

^{1}H NMR and ^{13}C NMR Spectrum of **2aa**

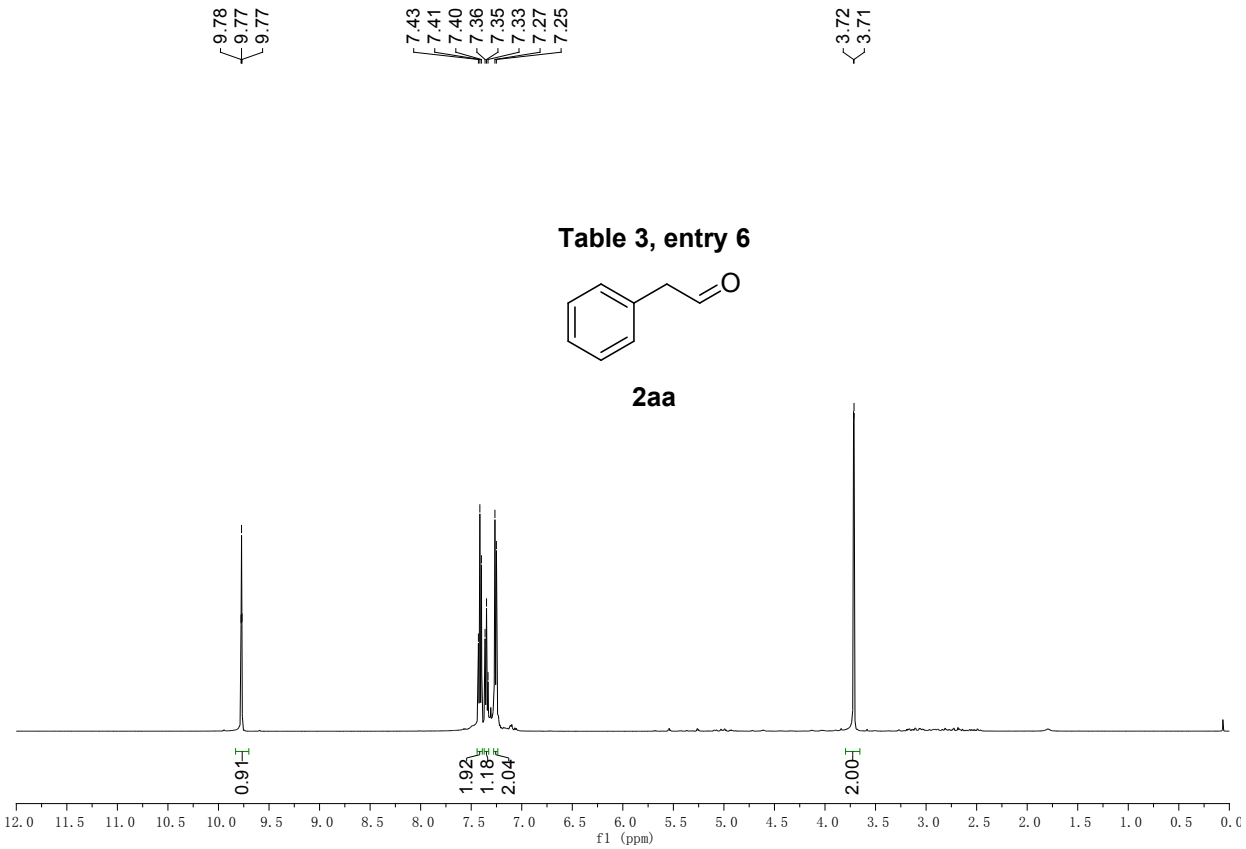

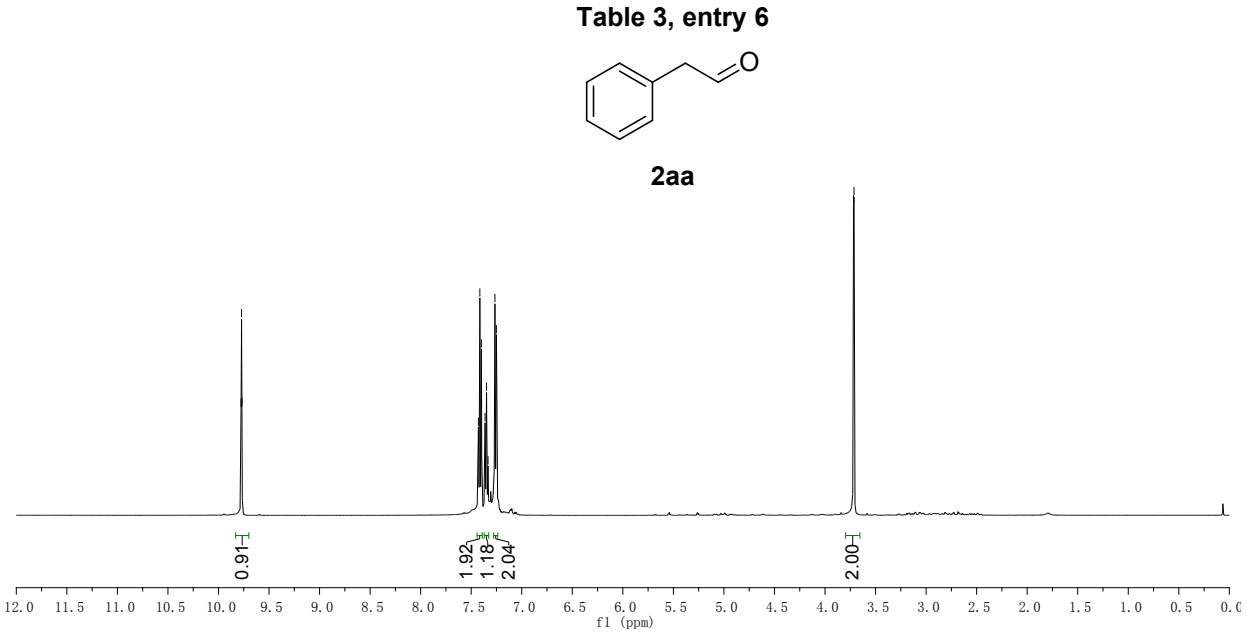

^{1}H NMR and ^{13}C NMR Spectrum of **2ab**

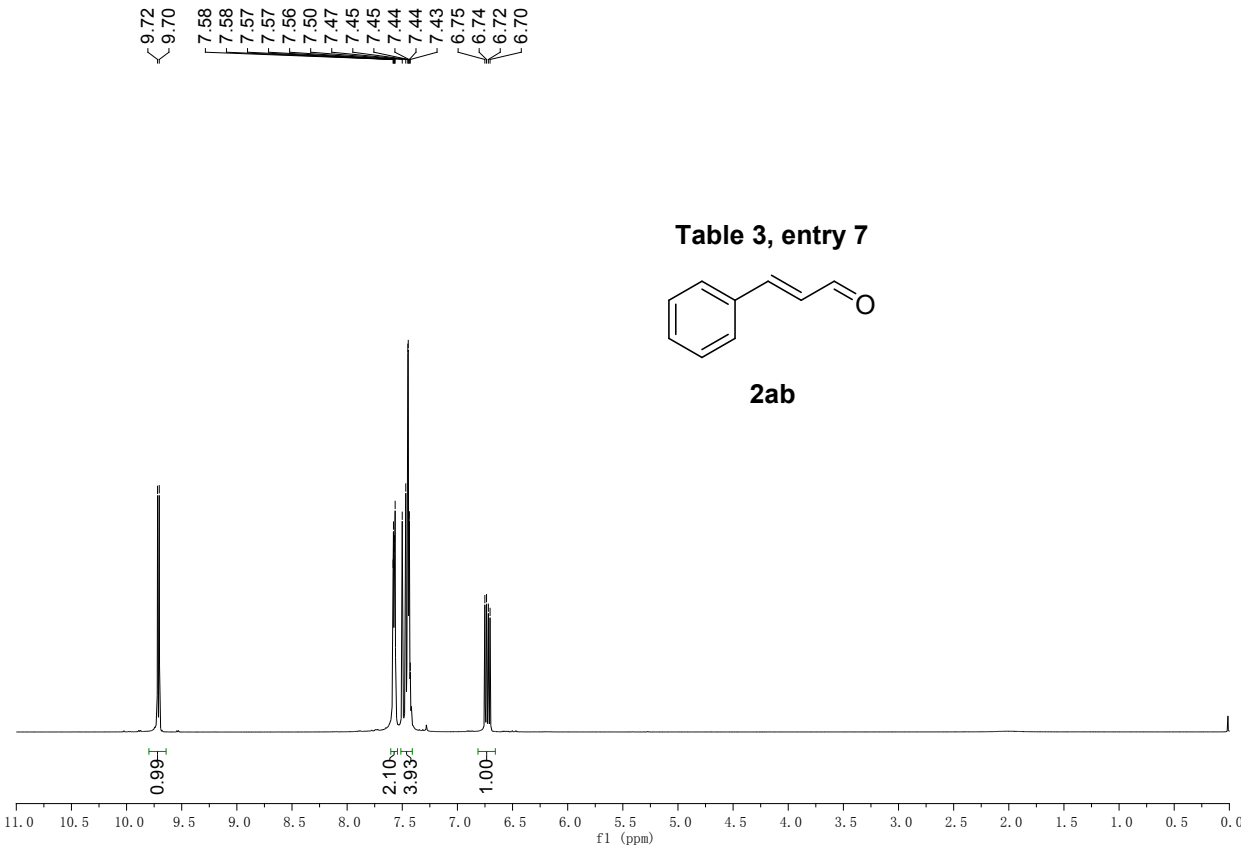

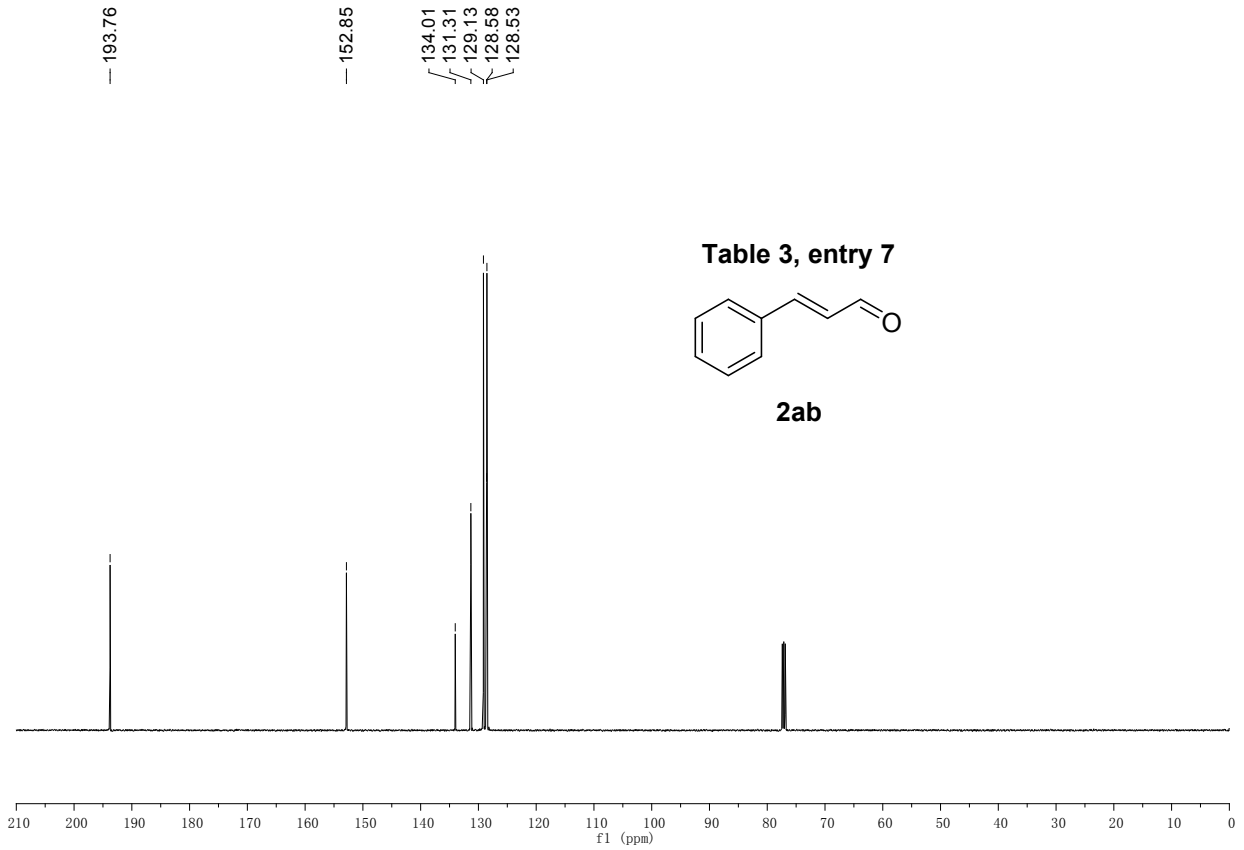

References:

1. (a) A. D. Becke, Density-Functional Thermochemistry. III. The Role of Exact Exchange. J. Chem. Phy., 1993, 98, 5648–5652; (b) C. Lee, W. Yang, R. G. Parr, Development of the Colle-Salvetti Correlation-Energy Formula into a Functional of the Electron Density. Phy. Rev. B, 1988, 37, 785–789.

2. W. J. Hehre, R. Ditchfield, J. A. Pople, Self-Consistent Molecular Orbital Methods. XII. Further Extensions of Gaussian-Type Basis Sets for Use in Molecular Orbital Studies of Organic Molecules. J. Chem. Phys., 1972, 56, 2257–2261.

3. P. J. Hay, W. R. Wadt, Ab initio Effective Core Potentials for Molecular Calculations. Potentials for the Transition Metal Atoms Sc to Hg. J. Chem. Phy., 1985, 82, 270–283.

4. M. J. Frisch, G. W. Trucks, H. B. Schlegel, G. E. Scuseria, M. A. Robb, J. R. Cheeseman, G. Scalmani, V. Barone, B. Mennucci, G. A. Petersson, H. Nakatsuji, M. Caricato, X. Li, H. P. Hratchian, A. F. Izmaylov, J. Bloino, G. Zheng, J. L. Sonnenberg, M. Hada, M. Ehara, K. Toyota, R. Fukuda, J. Hasegawa, M. Ishida, T. Nakajima, Y. Honda, O. Kitao, H. Nakai, T. Vreven, J. A., Jr. Montgomery, J. E. Peralta, F. Ogliaro, M. Bearpark, J. J. Heyd, E. Brothers, K. N. Kudin, V. N. Staroverov, R. Kobayashi, J. Normand, K. Raghavachari, A. Rendell, J. C. Burant, S. S. Iyengar, J. Tomasi, M. Cossi, N. Rega, J. M. Millam, M. Klene, J. E. Knox, J. B. Cross, V. Bakken, C. Adamo, J. Jaramillo, R. Gomperts, R. E. Stratmann, O. Yazyev, A. J. Austin, R. Cammi, C. Pomelli, J. W. Ochterski, R. L. Martin, K. Morokuma, V. G. Zakrzewski, G. A. Voth, P. Salvador, J. J. Dannenberg, S. Dapprich, A. D. Daniels, Ö. Farkas, J. B. Foresman, J. V. Ortiz, J. Cioslowski, D. J. Fox, In Gaussian 09, Revision B.01, Gaussian, Inc., Wallingford CT, 2009.

5. J. H. Liu, Y. W. Zhang, L. L. Lu, G Wu and W. Chen, Chem. Commun., 2012, 48, 8826−8828.